

Investigating the salinization and freshening processes of coastal groundwater resources in Urmia aquifer, NW Iran

Vahab Amiri · Mohammad Nakhaei · Razyeh Lak · Majid Kholghi

Received: 24 February 2015 / Accepted: 14 March 2016 / Published online: 21 March 2016
© Springer International Publishing Switzerland 2016

Abstract This paper presents the results of an assessment about interaction between Urmia Lake (UL) and coastal groundwater in the Urmia aquifer (UA). This aquifer is the most significant contributor to the freshwater supply of the coastal areas. The use of hydrochemical facies can be very useful to identify the saltwater encroachment or freshening phases in the coastal aquifers. In this study, the analysis of salinization/freshening processes was carried out through the saturation index (SI), ionic deltas (Δ), binary diagrams, and hydrochemical facies evolution (HFE) diagram. Based on the Gibbs plot, the behavior of the major ions showed that the changes in the chemical composition of the groundwater are mainly controlled by the water-soil/rock interaction zone and few samples are relatively controlled by evaporation. A possible

explanation for this phenomenon is that the deposited chloride and sulfate particles can form the minor salinity source in some coastal areas when washed down by precipitation. The SI calculations showed that all groundwater samples, collected in these periods, show negative saturation indices, which indicate undersaturation with respect to anhydrite, gypsum, and halite. In addition, except in a few cases, all other samples showed the undersaturation with respect to the carbonate minerals such as aragonite, calcite, and dolomite. Therefore, these minerals are susceptible to dissolution. In the dry season, the SI calculations showed more positive values with respect to dolomite, especially in the northern part of UA, which indicated a higher potential for precipitation and deposition of dolomite. The percentage of saltwater in the groundwater samples of Urmia plain was very low, ranging between 0.001 and 0.79 % in the wet season and 0.0004 and 0.81 % in the dry season. The results of HFE diagram, which was taken to find whether the aquifer was in the saltwater encroachment phase or in the freshening phase, indicated that except for a few wells near the coast, there is very little hydraulic interaction between UA and UL. In this coastal area, most of the samples that were collected repeatedly in both wet and dry seasons showed the same hydrochemical facies, which suggested that the seasonal groundwater fluctuations cannot significantly change the chemical composition of groundwater.

V. Amiri (✉) · M. Nakhaei
Department of Applied Geology, Faculty of Earth Sciences,
Kharazmi University, P.O. Box: 31979-37551, Tehran, Iran
e-mail: vahab.amiri@gmail.com

M. Nakhaei
e-mail: nakhaei@khu.ac.ir

R. Lak
Research Institute for Earth Sciences, Geological Survey of Iran,
Tehran, Iran
e-mail: lak_ir@yahoo.com

M. Kholghi
Department of Irrigation and Reclamation Engineering, Faculty of
Agriculture and Natural Resources, University of Tehran, Tehran,
Iran
e-mail: kholghi@ut.ac.ir

Keywords Hydrochemistry · Saltwater intrusion · Groundwater · Urmia Lake

Introduction

In many coastal regions, groundwater is a significant source of water supply for domestic, industrial, and agricultural purposes. On the other hand, saline/saltwater intrusion into fresh groundwaters is one of the main concerns in coastal aquifers around the world (Ozler 2003; Terzic' et al. 2008; Lucas et al. 2010; Mollema et al. 2013; Chen and Jiao 2014; Boluda-Botella et al. 2014). Salinization of groundwater by saline/saltwater intrusion is a widespread natural threat for many coastal aquifers around the world. In coastal lands, high extraction of groundwater can drop the water table of aquifer, decrease the freshwater pressure and help saline/saltwater to move inland, and initiate deterioration of coastal groundwater quality (Barker et al. 1998; Barlow and Reichard 2010).

The identification of major controlling mechanisms of water chemical composition and dynamics of flow systems is necessary to optimal management of coastal aquifers. Therefore, some information about groundwater chemistry, quality of groundwater for various purposes, recognition of different groundwater resources, and assessment of main chemical processes in such aquifers should be provided (Singh et al. 2009; Vandenbohede and Lebbe 2012; Skrzypek et al. 2013; Amiri et al. 2014, 2015; Matiatos et al. 2014; Esmaeili-Vardanjani et al. 2015). Groundwater salinization in coastal aquifers may occur due to saline/saltwater encroachment, but it may additionally encompass a range of complex geochemical processes that control the chemical composition of groundwater; for example, mixing of different water bodies in aquifer, water-rock interaction, and anthropogenic contamination of soil and water (Han et al. 2014).

Saline/saltwater encroachment into coastal fresh groundwaters depends on some factors, including surface and underground topography, hydraulic characteristics of aquifer, change in precipitation volume, groundwater flow patterns, infiltration rate, tidal and estuarine activity, and overexploitation of groundwater (Saxena et al. 2004; Melloul and Collin 2006; Lee and Song 2007; Kim et al. 2009; Mondal et al. 2010).

Freshwater and saltwater interactions in coastal areas have been widely examined using hydrogeochemical approaches (El Yaouti et al. 2009; Mondal et al. 2011; Mollema et al. 2013; Gurunadha Rao et al. 2013; Petelet-Giraud et al. 2013; Tomaszekiewicz et al. 2014), geophysical methods (Choudhury et al. 2001; Wilson et al. 2006; Cimino et al. 2008; Morrow et al. 2010;

Asfahani and Abou Zakhem 2013), and isotopic approaches (Schiavo et al. 2009; Langman and Ellis 2010; Rodellas et al. 2012; Mongelli et al. 2013; Carreira et al. 2014; Han et al. 2014; Cary et al. 2015).

The differences in the chemical composition of saline groundwater originating from saltwater encroachment and saltwater displacement are critical in evaluating the sources and processes of water salinization in coastal aquifers (Yechieli et al. 2009; Russak and Sivan 2010). Salinization of groundwater due to saline/saltwater intrusion can be precisely examined using the water chemistry data along with hydrogeological assessments (e.g., Andersen et al. 2005; Jorgensen et al. 2008; Han et al. 2014).

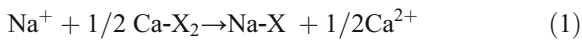
The present research was conducted in Urmia aquifer (UA). The study area is located on the west side of Urmia Lake (UL) in the NW of Iran. The UL is one of the largest hypersaline lakes in the world. This protected area is recognized as a biosphere reserve, based on UNESCO World Network of Biosphere Reserves (WNBR). In 1985, the UL had an area of about 5000 km², mean depth of 6 m, and an elevation of 1275.6 m above the mean sea level. It is located at the center of a vast drainage basin ($\approx 52,000$ km²), with all surface and groundwater draining toward UL. In recent years, the UL has faced a critical condition due to declining water level and increasing salinity (Ministry of Energy 2010). Currently, the lake floor is covered with a layer of salt. The salinity of this lake has increased dramatically in recent years because of some factors such as specific geological conditions, high evaporation rate, reduced inflow rate, and overexploitation of groundwater resources. The current situation of UL may have the irreparable environmental consequences such as damage to the surrounding fresh groundwater resources, agriculture, residents, animals, etc.

The hydrogeochemical status of Urmia coastal groundwaters has not been thoroughly studied. Therefore, there is little information about the chemical composition of groundwaters, controlling mechanisms of water chemistry, salinity problem, and interaction of UL and groundwater resources. The current study attempts to identify the chemical evolution of coastal groundwaters and possible interaction between UL and UA by using major ions and some trace element indicators. In other words, assessment of the intrusion and freshening processes and complex interactions between UL and fresh groundwater in the UA is carried out. In this study, the data included field observations and analysis of hydrochemical compositions of groundwater.

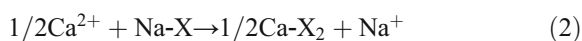
Theoretical approach

Exchange reactions

In coastal aquifers, there is a strong relationship between the saline/saltwater front movement and groundwater chemistry, because of the ion exchange process. Generally, fresh groundwater is dominated by calcium and bicarbonate ions originated mainly from the calcite dissolution. Under such conditions, the calcium can be adsorbed on the surfaces of ion exchangers such as fine-grained sediments and organic matter. On the other hand, sodium is the dominant sorbed cation in cases that the sediments are in contact with saline/saltwater (Sayles and Mangelsdorf 1977). When saline/saltwater encroaches on a coastal aquifer, sodium substitutes part of the calcium on the surface of solid particles, as presented in the following equation (Bear et al. 2013):



where X is the natural ion exchanger. In such reactions, sodium (calcium) is taken up (released) by (into) the solid (aqueous) portion of aquifer and the chemical composition of solute changes from NaCl- to CaCl₂-type water (Appelo and Postma 2005). In this reaction, the Cl⁻ concentration does not change, so it can be considered as a conservative ion. Therefore, as saline/saltwater encroaches to the coastal fresh groundwater, the Na⁺/Cl⁻ ratio decreases and the (Ca²⁺ + Mg²⁺)/Cl⁻ ratio increases. Under such conditions, the enrichments in Ca²⁺ and Mg²⁺ need to balance by the depletion of Na⁺ (i.e., Ca²⁺ + Mg²⁺ = -Na⁺), and therefore, a reverse process takes place by the influx of fresh groundwater (Bear et al. 2013):



The freshwater intrusion (flushing) into mixing zone leads to adsorption of Ca²⁺ and Mg²⁺ by the ion exchangers with concurrent release of Na⁺. This process can increase the Na⁺/Cl⁻ value and decrease the (Ca²⁺ + Mg²⁺)/Cl⁻ ratio and formation of NaHCO₃-type water. Therefore, water quality can show variations of saline/saltwater-freshwater mixing zone, and changing the ionic ratios indicates the dynamics of ion exchange. Based on laboratory studies, exchanges of Na⁺/Ca²⁺ and Ca²⁺/Na⁺ are the main controlling processes of the chemical composition of coastal groundwater in an alluvial aquifer affected by saline/saltwater encroachment. These changes occur in equilibrium with the carbonate

and sulfate (e.g., calcite and gypsum) minerals. Other processes include dolomitization-dedolomitization compelled by sulfate solution (causing an excess of calcium, magnesium, and sulfate), sulfate reduction (deficit of sulfate), and precipitation of gypsum coupled with ion exchange during the early stages of saline/saltwater encroachment.

Change of hydrochemical facies in the saline/saltwater encroachment and freshening processes

The hydrochemical facies evolution (HFE) diagram, which was proposed by Giménez-Forcada (2010) for the classification of water in coastal areas, considers just the percentage of the major cations (Ca²⁺ and Na⁺) and anions (HCO₃⁻, SO₄²⁻, and Cl⁻) which determine the dynamics of saline/saltwater encroachment. To simplify the complex processes, some less important considerations should be ignored. This occurs when the discussion does not take into account the ions occupying a secondary position in the freshwater and saline/saltwater end members, as is the case with SO₄²⁻, Mg²⁺, and K⁺ (Ghiglieri et al. 2012).

The sulfate percentage can be considered an alternative to bicarbonate percentage because both of these major anions are found in large quantities in freshwater. Because of the irregular behavior of Mg²⁺ ion, this cation is not considered in the exchange processes. In addition, due to the lower concentration of potassium than sodium in most cases, the sodium percentage incorporates the potassium percentage. The facies is determined as a function of the percentage of Ca²⁺ and Na⁺ cations: HCO₃⁻ (or SO₄²⁻) and Cl⁻ anions with respect to the sum of cations and anions, respectively. When the cation or the anion proportions are <0.5 but are higher than for any of the other cations and anions considered, the facies form is termed *Mix*. Triangular diagrams are the most widely used graphical representations of hydrochemical facies. In such diagrams, the ion concentrations (in meq/l) can be reported as percentages of the total anion and cation content. For representing the hydrochemical facies in the central part, the percentage of chloride and sulfate on the right side of triangle and calcium and magnesium on the left side of another triangle should be merged together. Therefore, the central part exhibits (%Cl⁻ + %SO₄²⁻) versus %HCO₃⁻, and (%Ca²⁺ + %Mg²⁺) versus (%Na⁺ + %K⁺) (Ghiglieri et al. 2012).

This problem can be resolved by representing the main processes occurring during the intrusion and freshening stages in the evolution of the hydrochemical facies

(Giménez-Forcada 2010). In HFE diagram (Fig. 1), the horizontal axis shows the percentages of Na^+ and Ca^{2+} in milliequivalents per liter, reproducing the exchange reactions. These percentages were calculated from the total sum of cations (including Mg^{2+}). The vertical axis shows the percentage of anions. The percentage of Cl^- represents saltwater, and percentage of HCO_3^- or SO_4^{2-} (depending on the dominant anion) represents freshwater composition. In the encroachment phase, increase in salinity (line I) initiates the reverse ion exchange reactions (line II). This event leads to the formation of Ca-Cl facies. Then, the groundwater chemistry moves (line III) toward the saline/saltwater composition (Na-Cl). In the freshening phase, freshwater recharge induces direct ion exchange reactions (lines I' and II'). This process leads to the formation of a Na- HCO_3 facies. Finally, the groundwater composition moves (line III') toward the composition of the freshwater that enables the recovery of the aquifer (Giménez-Forcada 2010).

Materials and methods

Study area

The Urmia plain, northwest of Iran, is located between the eastern longitude of $44^\circ, 20'$ and $45^\circ, 20'$ and

northern latitude of $37^\circ, 05'$ and $38^\circ, 05'$ (Fig. 2). UA is a large natural reservoir, which provides water requirements for different uses such as agricultural, industrial, and domestic. This convertible unconfined/confined aquifer has an area of around 868 km^2 . In this aquifer, groundwater flows from areas of a high hydraulic head in the west to the areas of a low hydraulic head in the east (next to UL). Four main rivers in this region (Nazlu-Chai, Rowzeh-Chai, Shahr-Chai, and Baranduz-Chai) originate from the western mountainous.

In this area, the geological units consist of the rock formations from Precambrian to Tertiary. The oldest rock units are composed mainly of volcanic series, acidic tuff, diorite, and gneiss. Tertiary rock units are formed mainly of different types of carbonate rocks (limestone and dolomite), conglomerate, sandstone, and shale (Kamei et al. 1973; Sartipi et al. 2014).

Based on the Global Bioclimatic Classification System, the Urmia plain is located in a Mediterranean pluvial seasonal-continental climate condition (Martinez et al. 1999). In the recent 30-year period, mean annual temperature and precipitation in the area are 11.52°C and 346.3 mm , respectively. In this period, mean maximum (31.2°C) and minimum (-6.1°C) temperatures are recorded in July and January, respectively (NOAA 2012; WMO 2014).

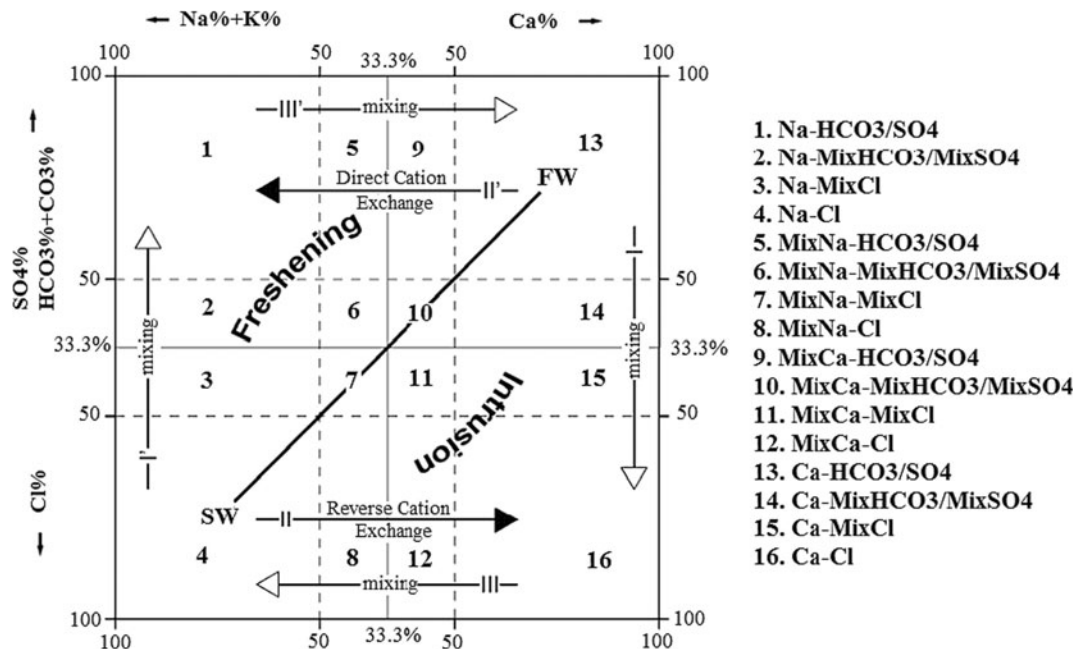


Fig. 1 HFE diagram (Giménez-Forcada 2010)

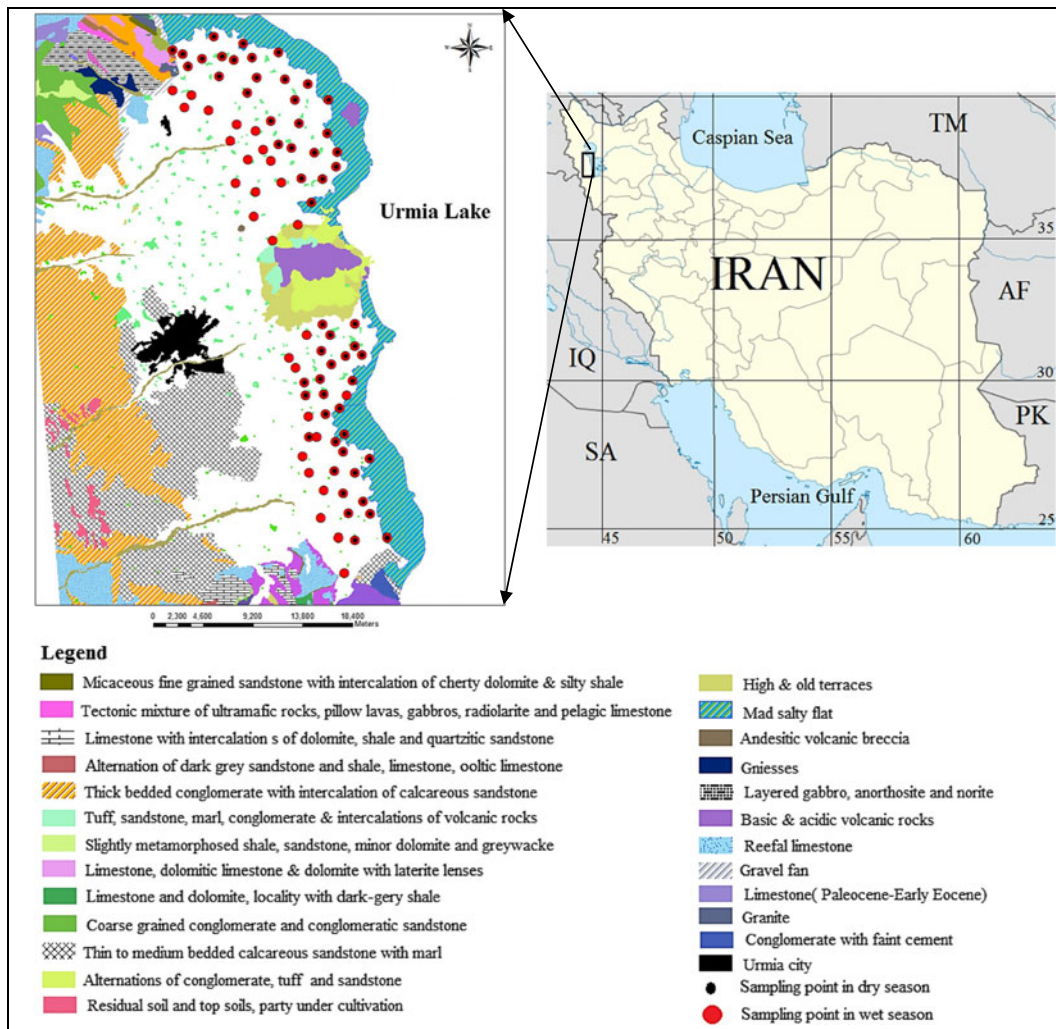


Fig. 2 Geological map of the study area, showing well locations

Water sampling and analyses

In this research, sampling of water from surface and underground resources is done in two stages: the first in June 2014 (as the wet season) and the second in September 2014 (as the dry season). The first and second phases of sampling were carried out on a network of 84 and 57 wells, respectively (Figs. 2 and 3). Groundwater samples were collected from shallow and deep boreholes and hand dug wells using standard sampling procedures (APHA 1985; ISO 1993). The depth of water wells and boreholes typically ranges from 10 to 120 m. In order to remove any stagnant water from the wells, about three casing volumes were pumped from the wells before commencing sampling.

At each sampling site, water samples were stored in two 250-ml polyethylene bottles after being filtered through 0.45-µm membrane filters. The water samples were divided into two distinct groups including non-acidified for anion analysis and acidified (with a few drops of Suprapur[®] nitric acid (HNO₃, 65 % v/v; Merck, Germany)) for analysis of cations and trace elements. The physical parameters such as Eh, pH, T, field salinity, dissolved oxygen (DO), and electrical conductivity (EC) were measured in the field by a HACH Multimeter device (Table 1). The samples were kept in an icebox and then transferred to a fridge (with an average temperature of 4 °C) until delivery to the laboratory for analysis (Table 1). Positions of sampling wells are shown in Figs. 2 and 3.

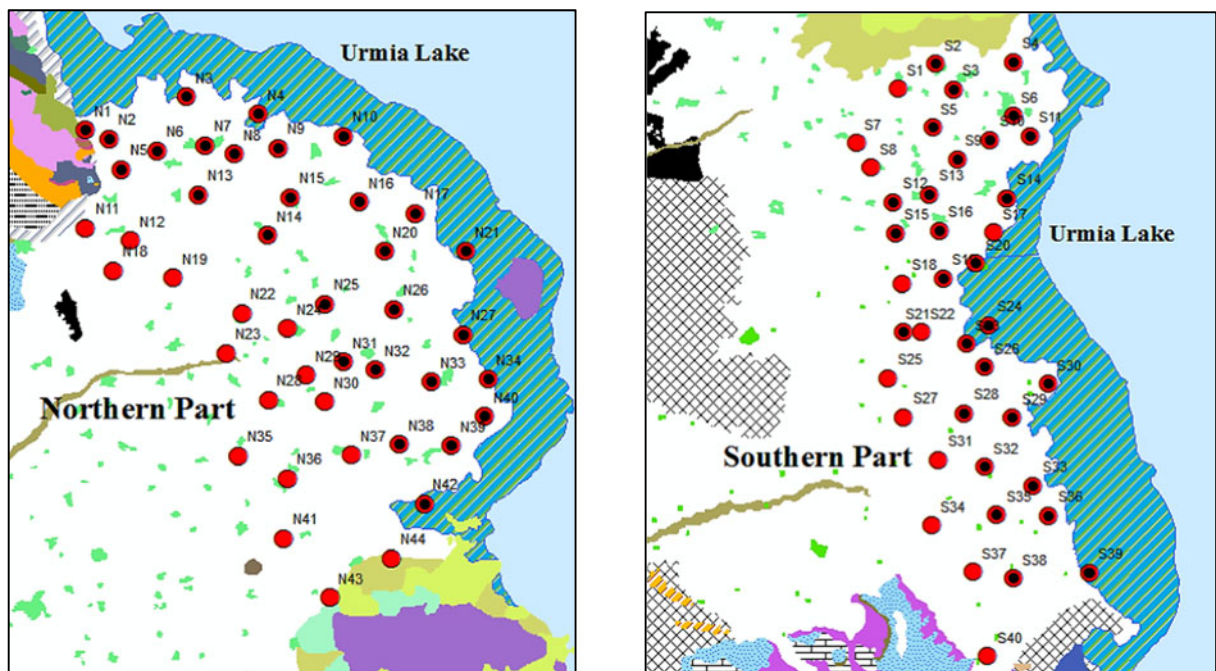


Fig. 3 Sampling points in the northern (*left*) and the southern (*right*) parts of UA. Red and black points are the groundwater samples collected in wet and dry seasons, respectively

Multivariate assessments

Twenty-one physicochemical variables (including temperature, pH, Eh, DO, EC, field salinity, Ca^{2+} , Mg^{2+} , Na^+ , K^+ , HCO_3^- , CO_3^{2-} , Cl^- , SO_4^{2-} , NO_3^- , NO_2^- , PO_4^{3-} , F^- , Br^- , B, and SiO_2) and 141 samples were analyzed using multivariate statistical techniques. In this research, the relationships between the variables were explored using Pearson's correlation coefficient with two statistical significance levels. The variable values (Table 1) were standardized prior to performing the multivariate analysis. Standardization of data set reduces the impact of different units of measurement and makes the data dimensionless (Liu et al. 2003). In this study, two of the most common multivariate statistical tools including the principal component analysis (PCA) and the hierarchical cluster analysis (HCA) were used for the analysis of the data set.

The PCA was used to interpret the structure of the original data set via a reduced new set of non-correlated variables (principal components (PCs)). In addition to significant data reduction, PCs can describe the variability of data set without losing much original information. The eigenvalues greater than 1 are considered for extraction of factors (Kaiser 1958; Harman 1960). The Kaiser's varimax rotation scheme (Kaiser 1958) is used for rotation of initial factors to the final factor.

In HCA technique, the variables are classified into different clusters based on similarities within a cluster and dissimilarities between different clusters. In this study, R-model hierarchical agglomerative cluster analysis is performed on the normalized data set by squared Euclidean distances and Ward's method (Ward 1963) to obtain dendrograms (Chen et al. 2007; Li et al. 2009). These methods have been successfully used for the assessment of groundwater chemistry by many researchers. The statistical assessments were done using SPSS 19.0 (IBM, Chicago, IL, USA).

Analysis the freshening/salinization processes and water-rock interaction

Analysis the freshening/salinization processes is carried out through the saturation index (SI), ionic deltas (Δ), binary and HFE diagrams. The SI is a valuable measure to determine whether the groundwater is saturated, undersaturated, or super-saturated with respect to the particular mineral. In aqueous solution, the saturation indices are calculated by using the approach illustrated by Appelo and Postma (2005). It is useful for assessing the extent to which groundwater chemistry was controlled by equilibrium with solid-phase minerals. PHREEQC

Table 1 Physicochemical parameters of the groundwater and UL water sampled in the wet season (June 2014) and dry season (September 2014) survey

	Wet season (June 2014)						Dry season (September 2014)					
	Groundwater			UL			Groundwater			UL		
	Min.	Max.	Ave.	Min.	Max.	Ave.	Min.	Max.	Ave.	Min.	Max.	Ave.
T	14	20	16.67	22	22.7	22.7	13.5	23	20	23	24	23.5
pH	6.87	8.42	7.24	6.35	6.41	6.38	6.98	8.92	8.3	6.55	6.6	6.57
Eh	-62.87	26.08	4.84	n.m.	n.m.	n.m.	-88	0.6	-75.8	n.m.	n.m.	n.m.
DO	0.58	4.5	1.16	n.m.	n.m.	n.m.	0.07	3.6	1.85	n.m.	n.m.	n.m.
EC	355	3800	1171.89	127,900	133,950	130,800	428	7180	1505.4	187,380	192,500	189,940
Field salinity	0.1	2	0.58	n.m.	n.m.	n.m.	0.21	3.6	0.24	n.m.	n.m.	n.m.
Ca ²⁺	3.54	319.9	105.11	113.2	130.7	121.27	6.11	271.5	105.6	57.4	57.9	57.65
Mg ²⁺	5.67	485.8	78.48	62,500	65,550	64,343.64	15.6	345	79	40,420	40,518	40,469
Na ⁺	15.5	1080.7	130.38	51,000	58,770	54,827.27	12.2	1229	177.89	9850	9877	9863.5
K ⁺	0.78	114.63	10.39	12,730	13,800	13,279.09	2.6	118.8	10.44	17,920	17,987	17,953.5
HCO ₃ ⁻	15.9	10,132.1	402.95	7191.8	9205.5	7984.18	30.2	734.4	306.51	13,664.3	13,685.4	13,674.85
CO ₃ ²⁻	24.7	605.5	103.34	7073.9	9054.5	7853.27	93.5	625.3	213.85	21,504.5	21,675	21,589.75
Cl ⁻	6.1	1325	116.23	160,443.6	175,811.8	166,870.3	7.4	2061.4	200.69	252,687.2	253,585.1	253,136.2
SO ₄ ²⁻	1	980	153.95	2900	3200	3036.36	1	590	143.63	56,000	56,700	56,350
NO ₃ ⁻	0.128	97	11.39	5.5	20.38	10.78	0.08	79.3	8.75	277	280	278.5
NO ₂ ⁻	0.003	0.34	0.01	0.003	0.007	0.0045	0.003	2.37	0.27	0.007	0.01	0.0085
PO ₄ ³⁻	0.07	6.3	0.44	1.8	9.2	3.4	0.05	5.9	0.54	6.7	6.82	6.76
F ⁻	0.16	5.7	1.17	202	236	216	0.11	4	1	24.5	25.3	24.9
Br ⁻	0.32	5.05	1.39	4.65	7.25	5.94	0.23	9.65	2.79	9.52	9.68	9.6
B	0.3	64	2.98	250	720	470	0.8	25.6	2.29	46	46.8	46.4
SiO ₂	5.14	37.28	11.17	1	1.2	1.10	3.57	33.31	10.5	0	0.4	0.2

Cations and anions are in milligram per liter, temperature (T) is in degree Celsius, field salinity is in part per thousand (ppt or ‰), electrical conductivity (EC) is in micro-Siemens per centimeter, and redox potential (Eh) is in millivolts

DO dissolved oxygen, *Min.* minimum, *Max.* maximum, *Ave.* average, *n.m.* not measured

version 2 (Parkhurst and Appelo 1999) is applied to determine the thermodynamic equilibrium SI for mineral species in the groundwater samples.

In order to determine the extent of saline/saltwater encroachment, a theoretical mixture percentage is calculated considering Cl⁻ as a conservative ion (i.e., not affected by ion exchange process). So, by considering this fact that the current investigation was carried out in an aquifer adjacent to a salt lake (UL), the saline/saltwater contribution (*x*) in a groundwater sample can be estimated using the following equation (Appelo and Postma 2005):

$$x = \frac{C_{Cl, sample} - C_{Cl, fresh}}{C_{Cl, lake} - C_{Cl, fresh}} \times 100 \tag{3}$$

where *C*_{Cl, sample} is the Cl⁻ content of the groundwater sample, *C*_{Cl, lake} is the Cl⁻ concentration of the UL, and

*C*_{Cl, fresh} indicates the Cl⁻ concentration of the fresh groundwater.

In this study, the lowest measured value of the Cl⁻ is considered to choosing the freshwater sample. Generally, the Cl⁻ does not remove from the system because of its high solubility (Appelo and Postma 2005). It can be originated not only from the aquifer matrix salts but also from a salinization source like saline/saltwater encroachment, etc. (Kouzana et al. 2009). Once calculated, the salt lake water fraction is used to calculate the theoretical concentration of each ion *i* resulting from the conservative mixing of UL water and the freshwater:

$$C_{i, mix} = (x/100) \times C_{i, lake} + (1-(x/100)) \times C_{i, fresh} \tag{4}$$

where *C*_{*i*, lake} and *C*_{*i*, fresh} are the concentrations of the ion *i* in UL water and fresh groundwater, respectively. The

ionic deltas (Δ) for each ion i resulting from some chemical reaction occurring with saline/saltwater-groundwater mixing are equal to the difference between the concentration of the conservative mixing $C_{i,mix}$ and the measured one $C_{i,sample}$ (Fidelibus et al. 2003):

$$\Delta C_i = C_{i,sample} - C_{i,mix} \quad (5)$$

The negative and positive values of ΔC_i indicate that groundwater sample is getting depleted or enriched, respectively, for ion i compared to the theoretical mixing value (Zghibi et al. 2013). In other words, positive ionic deltas specify enrichment because of some processes such as mineral dissolution or cation exchange reaction. The values close to zero show that the ion concentration is a result of conservative mixing.

Results and discussion

Groundwater chemistry

The result of chemical analyses and field measurements for 141 groundwater samples (84 samples in the wet season and 57 samples in the dry season) and 11 samples from UL (9 samples in the wet season and 2 samples in the dry season) is summarized in Table 1. In wet and dry seasons, the groundwater samples had average temperatures during sampling of around 17 and 20 °C, respectively. In wet and dry seasons, the pH values varied from 7.24 to 8.3 and Eh values from 4.84 to -75.8 mV, respectively. In the wet season, EC varied considerably from 355 to 3800 $\mu\text{S}/\text{cm}$ and in dry season changes from 428 to 7180 $\mu\text{S}/\text{cm}$.

As shown in Table 1, the average concentration of some hydrochemical parameters such as F^- , NO_3^- , SO_4^{2-} , HCO_3^- , Ca^{2+} , and field salinity in the wet season is more than in the dry season. During the wet season, the water table of coastal areas is higher than the dry season. Thus, dissolution rate will be more in the aquifer. In addition, by considering the 6-month residence time at the end of the wet season with higher rainfall and discharge, there is a greater chance for alkali and alkaline earth elements to be washed and transported in aqueous solutions. In fact, it is because of ionic potential of abovementioned elements, which makes them to form dissolved hydroxides soluble in water.

Statistical screening of groundwater data correlation matrix

Table 2 presents the correlation coefficient matrix for all physicochemical parameters. If the correlation coefficient (r) is greater than 0.7 or is between 0.5 and 0.7, it indicates the strongly and moderate correlation of two parameters, respectively.

In the wet season, parameters having high degrees of correlations are EC and Cl^- ($r=0.95$), EC and Na^+ ($r=0.90$), EC and Mg^{2+} ($r=0.79$), Na^+ and Cl^- ($r=0.90$), Cl^- and Mg^{2+} ($r=0.76$), Cl^- and K^+ ($r=0.78$), Na^+ and Mg^{2+} ($r=0.79$), Mg^{2+} and K^+ ($r=0.79$), SO_4^{2-} and NO_3^- ($r=0.73$), and Ca^{2+} and Eh ($r=0.77$). Other relations between parameters fall in the range of moderate to low correlations.

In the dry season, parameters having high degrees of correlations are EC and Cl^- ($r=0.92$), EC and Na^+ ($r=0.87$), EC and Mg^{2+} ($r=0.87$), EC and K^+ ($r=0.74$), Br^- and Mg^{2+} ($r=0.78$), Na^+ and Mg^{2+} ($r=0.78$), Na^+ and Cl^- ($r=0.78$), Mg^{2+} and SO_4^{2-} ($r=0.71$), Mg^{2+} and Cl^- ($r=0.77$), K^+ and Cl^- ($r=0.87$), Ca^{2+} and SO_4^{2-} ($r=0.79$), and Ca^{2+} and Eh ($r=0.80$).

This matrix indicates that (1) high correlation between Cl^- , Na^+ , Mg^{2+} , and EC reflects the significant contribution of these elements to the acquisition of the mineralization of water; (2) the high correlation between Na^+ and Cl^- indicates that the dissolution of halite is an important process of mineralization or Urmia saltwater intrusion is expected; (3) the relatively high correlation between Ca^{2+} and SO_4^{2-} shows that the process of base exchange with clay minerals has not high impact on dissolution of sulfate minerals; and (4) EC is not correlated with pH. This suggests that dissolution of the salts and other rock phases is not related to acidic conditions of groundwater, but it can be related to their solubility potential (Manno et al. 2006).

However, parameters having no significant correlations with other parameters are NO_2^- , HCO_3^- , B, SiO_2 , DO, and T in the wet season and NO_3^- , NO_2^- , PO_4^{3-} , CO_3^{2-} , B, SiO_2 , DO, and T in the dry season; therefore, these are not included in the subsequent multivariate analyzes.

Multivariate statistical analysis (PCA and HCA) and water-rock interactions

In this study, PCA is performed on the normalized data sets separately for the wet and dry seasons (Table 3). In wet and dry seasons, the first three and two components

Table 2 Pearson correlation matrix of physicochemical parameters in groundwater samples

	SO ₄ ²⁻	F ⁻	Cl ⁻	NO ₃ ⁻	NO ₂ ⁻	PO ₄ ³⁻	CO ₃ ²⁻	HCO ₃ ⁻	Ca ²⁺	K ⁺	Mg ²⁺	Na ⁺	Br ⁻	B	SiO ₂	EC	pH	Eh	DO	T
SO ₄ ²⁻	1.00	0.69 ^a	0.48 ^a				0.42 ^a	0.52 ^a	0.79 ^a	0.36 ^a	0.71 ^a	0.36 ^a	0.58 ^a			0.57 ^a	-0.49 ^a	0.68 ^a		
F ⁻	0.70 ^a	1.00	0.63 ^a				0.47 ^a	0.58 ^a	0.45 ^a	0.54 ^a	0.65 ^a	0.58 ^a	0.50 ^a			0.65 ^a			0.47 ^a	0.26 ^b
Cl ⁻	0.55 ^a	0.54 ^a	1.00					0.50 ^a	0.30 ^b	0.87 ^a	0.77 ^a	0.78 ^a	0.59 ^a			0.92 ^a			0.38 ^a	0.52 ^a
NO ₃ ⁻	0.73 ^a	0.56 ^a	0.39 ^a	1.00																
NO ₂ ⁻				1.00																
PO ₄ ³⁻		0.51 ^a			1.00				-0.28 ^b											
CO ₃ ²⁻			0.52 ^a			1.00			0.44 ^a		0.48 ^a	0.27 ^b						0.28 ^b	0.38 ^a	
HCO ₃ ⁻						1.00				0.45 ^a	0.43 ^a	0.37 ^a	0.31 ^b	0.36 ^a		0.48 ^a		0.28 ^b		
Ca ²⁺	0.67 ^a	0.34 ^a	0.33 ^a	0.52 ^a		-0.29 ^a	0.66 ^a	1.00			0.65 ^a	0.33 ^b	0.48 ^a	0.29 ^b		0.44 ^a		0.80 ^a		
K ⁺	0.24 ^b	0.29 ^a	0.78 ^a	0.16			0.55 ^a		0.33 ^a	1.00	0.63 ^a	0.57 ^a	0.41 ^a			0.74 ^a		0.42 ^a	0.41 ^a	0.39 ^a
Mg ²⁺	0.47 ^a	0.37 ^a	0.76 ^a	0.29 ^a			0.44 ^a		0.33 ^a	0.80 ^a	1.00	0.78 ^a	0.78 ^a	0.30 ^b		0.87 ^a		0.42 ^a	0.28 ^b	0.32 ^b
Na ⁺	0.59 ^a	0.63 ^a	0.90 ^a	0.33 ^a			0.44 ^a		0.73 ^a	0.73 ^a	0.79 ^a	1.00	0.67 ^a			0.87 ^a		0.27 ^b	0.28 ^b	0.46 ^a
Br ⁻	0.37 ^a	0.51 ^a	0.54 ^a	0.23 ^b			0.31 ^a		0.42 ^a	0.42 ^a	0.44 ^a	0.55 ^a	1.00			0.68 ^a		0.27 ^b		0.37 ^a
B			0.26 ^b								0.22 ^b	0.27 ^b	0.48 ^a	1.00		0.26 ^b				
SiO ₂	0.36 ^a	0.29 ^a	0.26 ^b	0.25 ^b							0.28 ^a	0.28 ^a	0.35 ^a		1.00				0.31 ^b	0.49 ^a
EC	0.70 ^a	0.65 ^a	0.95 ^a	0.51 ^a			0.44 ^a		0.44 ^a	0.70 ^a	0.79 ^a	0.90 ^a	0.56 ^a	0.25 ^b	0.29 ^a	1.00		0.26 ^b		
pH	-0.41 ^a			-0.35 ^a					-0.77 ^a							-0.22 ^b	1.00	-0.80 ^a		
Eh	0.41 ^a			0.35 ^a					0.77 ^a							0.22 ^b	-1.00 ^a	1.00		
DO										0.21 ^b									1.00	0.38 ^a
T												0.23 ^b		0.29 ^a	0.22 ^b				0.28 ^a	1.00

The correlation coefficients for the wet and dry seasons are presented in down and upper triangular, respectively

^a Significance at the 0.01 probability level

^b Significance at the 0.05 probability level

Table 3 The rotated loadings, the eigenvalues for each factor, the percentage of variance, and the total cumulative percentage of variance for wet and dry seasons

parameter	Wet season			Dry season	
	RC1	RC2	RC3	RC1	RC2
SO ₄ ²⁻		0.80		0.52	0.74
F ⁻		0.90		0.73	
Cl ⁻	0.85			0.93	
NO ₃ ^{-a}		0.73		n.c.	n.c.
PO ₄ ³⁻			-0.76	n.c.	n.c.
CO ₃ ²⁻	0.80			n.c.	n.c.
HCO ₃ ^{-a}	n.c.	n.c.	n.c.	0.54	
Ca ²⁺		0.50	0.75		0.86
K ⁺	0.91			0.82	
Mg ²⁺	0.86			0.84	
Na ⁺	0.81			0.90	
Br ⁻	0.50			0.73	
EC	0.78	0.54		0.93	
pH			-0.94		-0.87
Eh			0.94		0.94
Eigenvalue	4.61	3.40	3.28	5.68	3.34
Total variance (%)	32.97	24.34	23.49	47.38	27.83
Cumulative variance (%)	32.97	57.31	80.80	47.38	75.21

Loadings with absolute values <0.5 were omitted

RCs rotated principal components, n.c. not considered

^aNO₃⁻, PO₄³⁻, and CO₃²⁻ not considered in dry and HCO₃⁻ in wet seasons

extracted have eigenvalues >1 and correspond to approximately 80.80 and 75.21 % of the total variance, respectively. The variance of the principal loadings is maximized by Varimax rotation. The principal component loadings for these parameters along with their variance and loading values (>0.5) are presented in Table 3.

In the wet season, the first rotated principal component (RC1) explains approximately 32.97 % of the total variance, exhibiting the strong-to-moderate positive association with Cl⁻, CO₃²⁻, K⁺, Mg²⁺, Na⁺, Br⁻, and EC. These parameters (except Br⁻) are the major ions in the aqueous solution. The increase in Cl⁻ content of some groundwater samples could be attributed to the mixing with some salinity sources such as UL water, which is characterized by a high Cl⁻ concentration. The positive correlation between EC and aforementioned variables suggests that this principal component can be considered as a salinization index (Liu et al. 2003). The moderate positive correlation between EC and Br⁻ concentrations ($r=0.56$) (Table 2) besides the weak correlation of these variables with EC in determined principal components (Table 3) shows that they cannot be regarded as a water salinization index attributed to saltwater intrusion. The presence of Br⁻ in groundwater samples can be associated with the presence of brackish water. On

the other hand, the saline groundwater samples do not show the high values of dissolved Br⁻, suggesting that enrichment in this parameter is not only due to mixing with saline surface/groundwater (Morell et al. 1986). The second principal component (RC2) which explains approximately for 24.34 % of total variance shows strong positive loadings on SO₄²⁻, F⁻, and NO₃⁻ and moderate loadings on Ca²⁺ and EC. As presented in Table 1, UL water with an average SO₄²⁻ concentration equal to 3036.36 mg/l can be regarded as a possible source of sulfate in groundwater samples. In this case, the potential impact of evaporite deposits and geological formations should be investigated. Generally, the release of the F⁻ into the groundwater occurs through the weathering of rocks and through deposition of atmospheric volcanic particles. Since the geology of the recharge zone (west of Urmia plain) is mainly composed of carbonate rocks, the Ca²⁺ ions release into the groundwater, which changes the pH in the RC2 and RC3 principal components. Infiltrating from farmlands and wastewater leaching from rural and urban areas are the major sources of nitrate in groundwater samples. Strong positive association with Ca²⁺ and Eh, as well as a strongly negative association with pH and PO₄³⁻, characterizes the third principal component (RC3) that

explains approximately 23.49 % of total variance. Despite the high concentration of PO_4^{3-} (Table 1) in the UL water, this parameter probably has not any impact on groundwater chemistry (negative correlation).

In the dry season, the first two RCs explained 75.21 % of the total variance in the data set (Table 3). The RC1 corresponds to approximately 47.38 % of total variance, showing strong-to-moderate positive association with SO_4^{2-} , F^- , Cl^- , HCO_3^- , K^+ , Mg^{2+} , Na^+ , Br^- , and EC. In this factor, the high positive loadings of Cl^- (0.93) and Na^+ (0.90) indicate the importance of main potential sources of these ions (i.e., UL). The strongly positive correlation of other parameters along RC1 (except SO_4^{2-}) could be attributed to mineralization of groundwater by water-soil/rock interaction. The strong positive correlation of Br^- as a conservative ion (Morell et al. 2008) indicates that in the dry season, bromide has more impact on water chemistry. Ged (2013) showed that increase in Br^- content of groundwater samples represents the degree of sea/saltwater encroachment into coastal aquifers. The second principal component (RC2) which explains approximately 27.83 % of the total variance displays strong positive loadings on SO_4^{2-} , Ca^{2+} , and Eh, as well as strong negative loading on pH. Like the wet season, calcium and sulfate are located in the second principal component. In comparison to the wet season, the correlation of SO_4^{2-} is lower and correlation of Ca^{2+} is higher in the dry season. The strong positive loading on Ca^{2+} in this component rather than the wet season shows the more impact of limestone dissolution on the groundwater chemistry. One reason for more importance of Ca^{2+} in the dry season can be attributed to groundwater extraction in eastern locations (near to UL) and movement of freshwater from the recharge zones (western mountains) to the eastern parts.

Although the PCA has proven to be more suitable for presentation of the sources of water chemistry changes than the HCA, use of a combination of these methods leads to a better understanding of the hydrochemistry (Yidana et al. 2008; Helena 2000). Based on HCA of water quality data, there were three distinct clusters of parameters in the wet season and two groups in the dry season (Fig. 4). In the wet season, clusters are relatively similar to results of PCA (Table 3), and in the dry season, parameters of two clusters are quite similar to the results of RC1 and RC2.

The presence of three and two distinct clusters in wet and dry seasons, respectively, suggests that there may be three and two distinct sets of influences that are affecting

water samples in this study area, i.e., a combination of natural factors, pollution, and other human activities (Zhang et al. 2014). In the wet season dendrogram, EC, Cl^- , Na^+ , K^+ , and Mg^{2+} and in the dry season dendrogram EC, Cl^- , Na^+ , and Mg^{2+} show the same changes and are located in a distinct sub-cluster. By considering the hydrogeological properties of the study area and the presence of UL at the east of the aquifer, we inferred that the influence on these sub-clusters is most likely the effect of mineral dissolution, because the concentrations of these elements increased with flow down the hydraulic gradient, from west to east, and saltwater encroachment from the UL side. Bromide with similar changes to other parameters can be interpreted as an indicator for saltwater intrusion in groundwater resources. Bromide is generally conservative in the groundwater systems, but Gerritse and George (1988) showed that, sometimes, bromide could be adsorbed on the organic substances and on mineral surfaces in groundwater with low pH value (Seaman et al. 1996). The ratio of chloride to bromide can be used to identify the freshwater-saltwater mixing process (Morell et al. 2008). Variables of other clusters in the wet and dry seasons cannot be attributed to a single factor. Many processes including natural processes such as evaporation and water-soil/rock interaction and anthropogenic sources such as agricultural activities may affect parameters of these clusters. In this cluster, the similarity of changes of some variables such as Ca^{2+} and SO_4^{2-} can persuade us to attribute the Ca^{2+} to weathering the geological carbonate formations in the west of Urmia plain and some sulfate unites (e.g., gypsum and anhydrite). By considering the very high concentration of sulfate in the UL water (an average of 3036.36 mg/l in the wet season and 56,350 mg/l in the dry season; Table 1), it can be considered as a potential source of SO_4^{2-} in the coastal groundwater samples.

In this research, Gibbs plots (Gibbs 1970) were used to obtain a better understanding of the impacts of hydrochemical processes such as precipitation, water-rock interaction, and evaporation-crystallization on groundwater chemistry. Gibbs suggested that some valuable information about controlling mechanisms of the groundwater chemistry can be provided by plotting the total dissolved solid (TDS) values against $\text{Na}^+ / (\text{Na}^+ + \text{Ca}^{2+})$ and $\text{Cl}^- / (\text{Cl}^- + \text{HCO}_3^-)$. Based on Gibbs plots (Fig. 5), the groundwater samples mostly located in the water-soil/rock interaction zone and some samples were close to the evaporation-crystallization dominance zone.

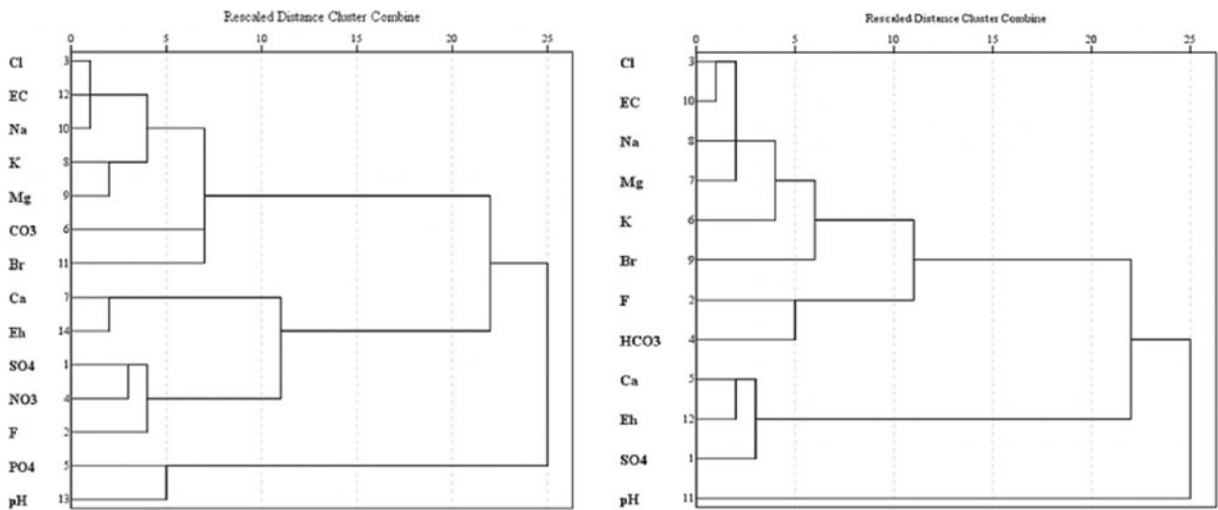


Fig. 4 Dendrogram showing the results of the HCA of parameters for wet (*left*) and dry (*right*) seasons

An explanation for this phenomenon is the spray of chloride and sulfate microparticles from the salty playas surrounding the UL. In such areas, the main aerosol particles (diameter >1 μm) are some common minerals (e.g., clays, calcite, and the rock-forming silicates), and other particles (diameter <1 μm) are sulfates and alkali and alkaline-earth salts (Schryer 1982). Observations indicate that the UL is dry for a large part of the year, so the vast portions of playas are exposed to wind erosion. By considering the composition of UL saltwater, it is expected that some chloride and sulfate microparticles be derived from salty playas. Therefore, the deposited particles form the minor salinity source in the some coastal areas when washed down by precipitation.

In this study, the geochemical interpretations are done by using the saturation index (SI) of minerals. Saturation coefficient values between -0.5 and 0.5 are considered as

equilibrium state. This index is used to assess the rate of groundwater saturation toward the mineral phases such as precipitation-crystallization and/or dissolution reactions occurring in groundwater systems (Bouzourra et al. 2015). Figure 6 and Table 4 represent the computed saturation indices of anhydrite, aragonite, calcite, dolomite, gypsum, halite, and fluorite with PHREEQC.

The calculations indicate that all groundwater samples have negative saturation indices, which show the undersaturation with respect to anhydrite, gypsum, and halite, indicating the subsequent dissolution of these minerals. In addition, except in some cases that are saturated with respect to dolomite (e.g., S30 and N40) and aragonite and calcite (N39), all other samples showed the undersaturation with respect to the carbonate minerals (e.g., aragonite, calcite, and dolomite). Therefore, the carbonate minerals are susceptible to

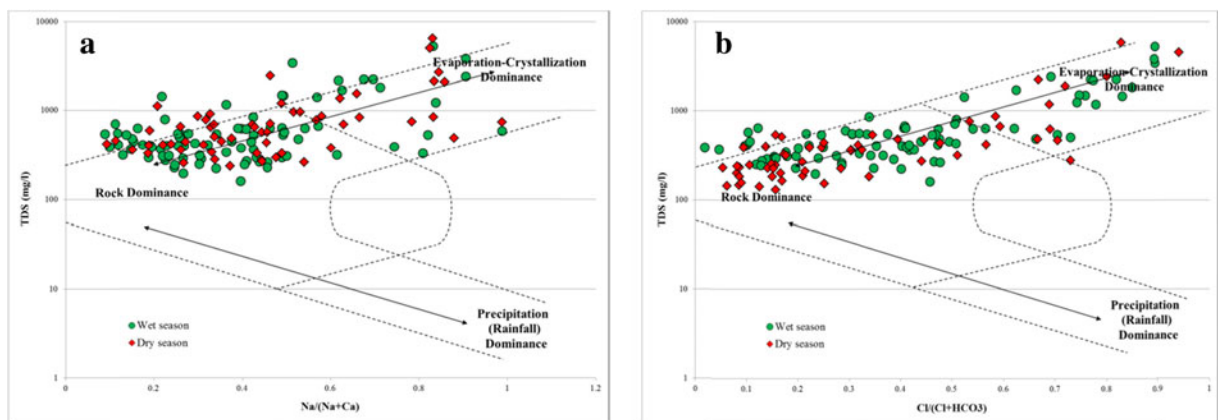


Fig. 5 Mechanisms controlling groundwater chemistry in UA

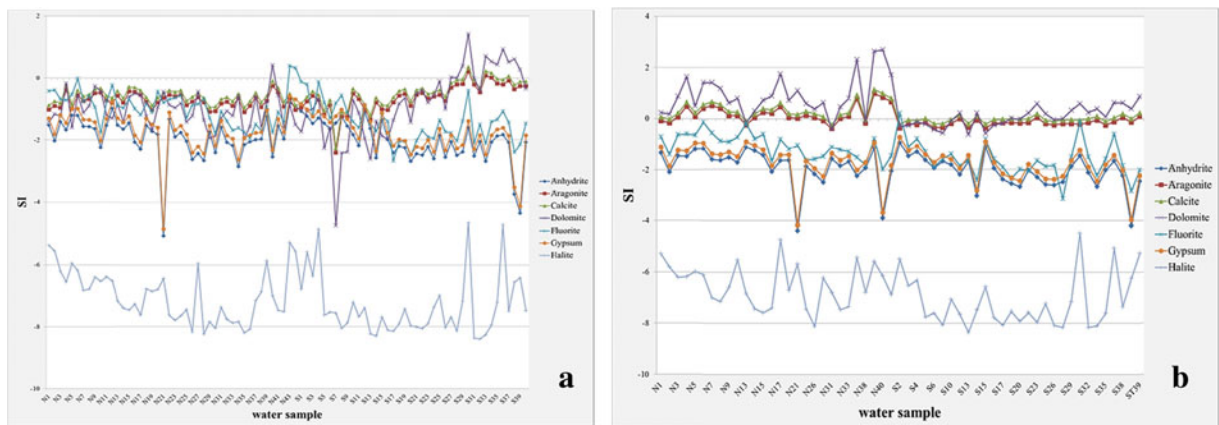


Fig. 6 Change of saturation indices (SI) of major phases in Urmia groundwater samples in **a** wet and **b** dry seasons

dissolution. In the dry season (September 2014), groundwater samples exhibited the higher positive SI values with respect to dolomite and relatively positive SI with respect to calcite and aragonite, especially in the northern part of UA, that indicate the higher potential for crystallization and deposition of dolomite, calcite, and aragonite. Therefore, the mentioned minerals are not prone to dissolution. Except for groundwater samples near the metamorphous rocks (S2 and N43), saturation indices with respect to fluorite are negative, which reveals the undersaturation conditions.

Evaluation of saltwater encroachment into the Urmia groundwater resources

Because of relatively conservative behavior of most halogens in aquifers, they are the most common tracers that have been extensively used to explain the salinity sources in groundwater systems. In general, the

conservative characteristic of Cl^-/Br^- ratio has been frequently used to determine the salinization processes (Mandilaras et al. 2008; Katz et al. 2011; Warner et al. 2013). Although the Cl^-/Br^- ratio has been illustrated as a tracer to identify the salinity origins in groundwater, Whittemore and Davis (1995) showed that the Cl^-/Br^- ratios in groundwater could be changed by sorption of Br^- on soil clay minerals and iron oxides. Other processes can modify the Cl^-/Br^- ratio in groundwater including organic matter decomposition that can release the Br^- into the groundwater, lateral encroachment of sea/saltwater, up-coning (vertical sea/saltwater encroachment) of brines, and fluids derived from dissolution of evaporite deposits (Katz et al. 2011). Although some salinity sources have characteristic high Cl^-/Br^- values (e.g., wastewater and evaporite dissolution) relative to other sources with low Cl^-/Br^- values (e.g., brines originated from evaporated seawater and animal waste), some overlaps may occur. In addition, the water

Table 4 Saturation indices of major phases in groundwater samples

Period		Anhydrite (CaSO ₄)	Aragonite (CaCO ₃)	Calcite (CaCO ₃)	Dolomite (CaMg(CO ₃) ₂)	Fluorite (CaF ₂)	Gypsum (CaSO ₄ ·2H ₂ O)	Halite (NaCl)
Wet season	Min. (no. of sample)	-5.07 (N21)	-2.4 (S7)	-2.26 (S7)	-4.74 (S7)	-2.67 (S17)	-4.85 (N21)	-8.41 (S32)
	Max. (no. of sample)	-0.8 (N43)	0.21 (S30)	0.35 (S30)	1.42 (S30)	0.39 (N43)	-0.58 (N43)	-4.66 (S30)
	Ave.	-1.98	-0.69	-0.54	-0.93	-1.18	-1.76	-7.17
Dry season	Min. (no. of sample)	-4.38 (N21)	-0.38 (N31)	-0.24 (N31)	-0.62 (S13)	-3.15 (S28)	-4.16 (N21)	-8.35 (S13)
	Max. (no. of sample)	-0.94 (S2)	0.99 (N39)	1.14 (N39)	2.69 (N40)	0.21 (S2)	-0.72 (S2)	-4.47 (S30)
	Ave.	-2.01	0.02	0.17	0.51	-1.35	-1.79	-6.84

movement in fine-grained and clay-rich sediments may change the Cl^-/Br^- values because of adsorption of bromide onto the solid surfaces at $\text{pH} < 7$ (Goldberg and Kabengi 2010). Therefore, the Br^- concentration may not always be considered as a conservative tracer in aquatic systems. Figure 7 presents the changes of Cl^-/Br^- ratio versus Cl^- concentration in the groundwater and UL samples. As shown, Cl^-/Br^- ratios for most samples collected in the wet season are higher than Cl^-/Br^- values determined for water samples collected in the dry season. Based on the calculations for wet season, there is a wide range of low Cl^-/Br^- ratios ≈ 1.6 (sample S31) and high Cl^-/Br^- ratios ≈ 900 (sample S3). In the dry season, lowest (≈ 3.2) and highest (≈ 442) Cl^-/Br^- ratios can be seen in samples N26 and ST39, respectively. In both wet and dry seasons, the most coastal groundwater samples show the high Cl^-/Br^- mass ratios and Cl^- concentrations.

In general, other sources of salinization (e.g., sewage disposal systems, livestock facilities, and fertilized cropland and gardens) should be taken into account to change the concentration of Cl^- , Br^- , and salinization in some wells. Based on McArthur et al. (2012), the contamination of groundwater systems by sewage can be discovered by the presence of NO_3^- and/or of SO_4^{2-} in values greater

than expected from marine contributions (i.e., $\text{NO}_3^-/\text{Cl}^-$ mass ratios > 0.0002 and $\text{SO}_4^{2-}/\text{Cl}^-$ mass ratios > 0.14). The inverse is not true; the absence of NO_3^- or SO_4^{2-} does not show that wastewater is absent because the reducing conditions in some coastal groundwater resources quickly remove both SO_4^{2-} and NO_3^- from recharge (e.g., Lowers et al. 2007; Buschmann and Berg 2009). In our study area, the $\text{NO}_3^-/\text{Cl}^-$ mass ratios in UL are equal to 0.0021 and 0.001, and the $\text{SO}_4^{2-}/\text{Cl}^-$ mass ratios are equal to 0.018 and 0.22 in wet and dry seasons, respectively. Based on the results, all groundwater samples collected in both seasons have greater $\text{NO}_3^-/\text{Cl}^-$ mass ratios than UL. In addition, about 98.81 and 91.23 % of collected groundwater samples in wet and dry seasons show the higher values of $\text{SO}_4^{2-}/\text{Cl}^-$ ratios than UL, respectively.

As an example, the Cl^-/Br^- ratio versus Cl^- concentration in sewage or septic tank (Panno et al. 2006; McArthur et al. 2012) and agricultural drainage (Schroeder and Rivera 1993) is presented in Fig. 7. Generally, the high concentration of nitrate in groundwater samples can be attributed to the wastewater (Nakhaei et al. 2015) or agricultural drainage (Amiri et al. 2015). In the wet and dry seasons, we found that some samples with high values of Cl^-/Br^- ratio vs. Cl^- concentration show the high NO_3^- content (e.g.,

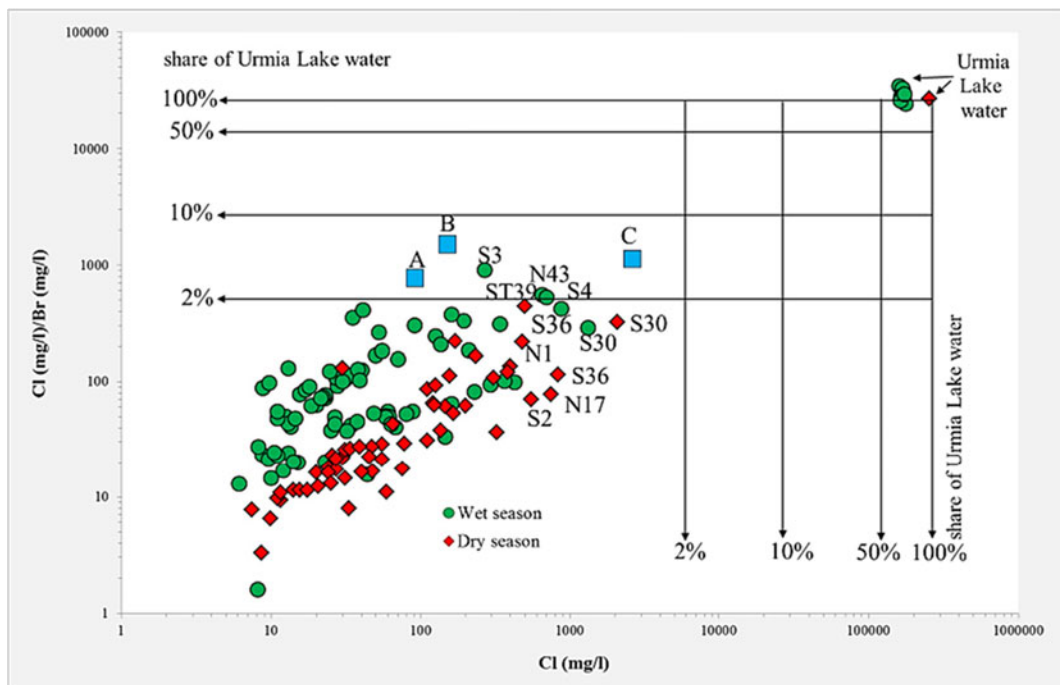


Fig. 7 Changes of Cl^-/Br^- ratio versus Cl^- concentration in groundwater and UL samples. Blue squares are the sewage or septic tank (A: Panno et al. (2006) and B: McArthur et al. (2012)) and agricultural drainage (C: Schroeder and Rivera (1993))

samples S30, S4, and N43 in the wet season and S30 and S39 in the dry season). It should be pointed out that just samples N43 and N44 in the wet season and S6 in the dry season exceed the maximum contaminant level for nitrate (50 mg/l) (WHO 2011).

Based on distribution of groundwater samples in Fig. 7, some samples are close to the chemical composition of sewage or septic tank and agricultural drainage effluents, but their impact cannot be precisely confirmed by our data and requires a comprehensive study to define the role of all possible factors. It should be noted that in this study, in order to reduce the adverse effect on water chemistry, an attempt was made to collect the samples from locations that are far from pollution sources such as sewage.

One of the useful halogens that can be used in exploring the saltwater intrusion and freshening of groundwater resources is boron. Boron in aquatic solutions occurs as uncharged boric acid ($B(OH)_3^0$) and borate ion ($B(OH)_4^-$) forms. In addition to base-exchange reactions, boron is typically adsorbed during saline/saltwater intrusion (Jones et al. 1999). Thus, the high Cl^-/B ratios (Fig. 8) in groundwater samples may characterize the Urmia saltwater encroachment. The results showed that boron and chloride are weakly correlated, but the relative boron enrichment in some groundwater samples, which have the high Cl^- concentration, is

apparent. The relative enrichment of boron relative to the conservative mixing direction between saltwater and freshwater indicates that boron is released from the adsorption sites. The relative enrichment of boron can be attributed to the re-equilibrium between adsorbed and dissolved boron during freshening processes which resulted in desorption of boron (Vengosh 2014). As a result, just some areas of the UA (e.g., S30, S36, N17, N43, ST39, S2, and S4) show evidence of saltwater originated from some possible sources such as UL and dissolution of salty playas (high Cl^-/B ratios) while others show evidence of freshening (low Cl^-/B ratios).

In order to the interpretation of dynamic characteristics of UL saltwater encroachment, we assessed several bivariate diagrams and the relationships between Ca^{2+} , Mg^{2+} , Na^+ , K^+ , SO_4^{2-} , and Cl^- . The major ion/chloride relationships for all the samples collected in both wet and dry seasons are plotted in Fig. 9, in which the conservative mixing of fresh groundwater and UL saltwater is presented as a line in each part.

The EC and Cl^- show a relatively linear correlation (Fig. 9a). This indicates that admixture with UL saltwater is one of the potential processes responsible for the salinization of groundwater samples, although the deviation of some samples from these lines suggests that some other processes such as water-soil/rock interaction

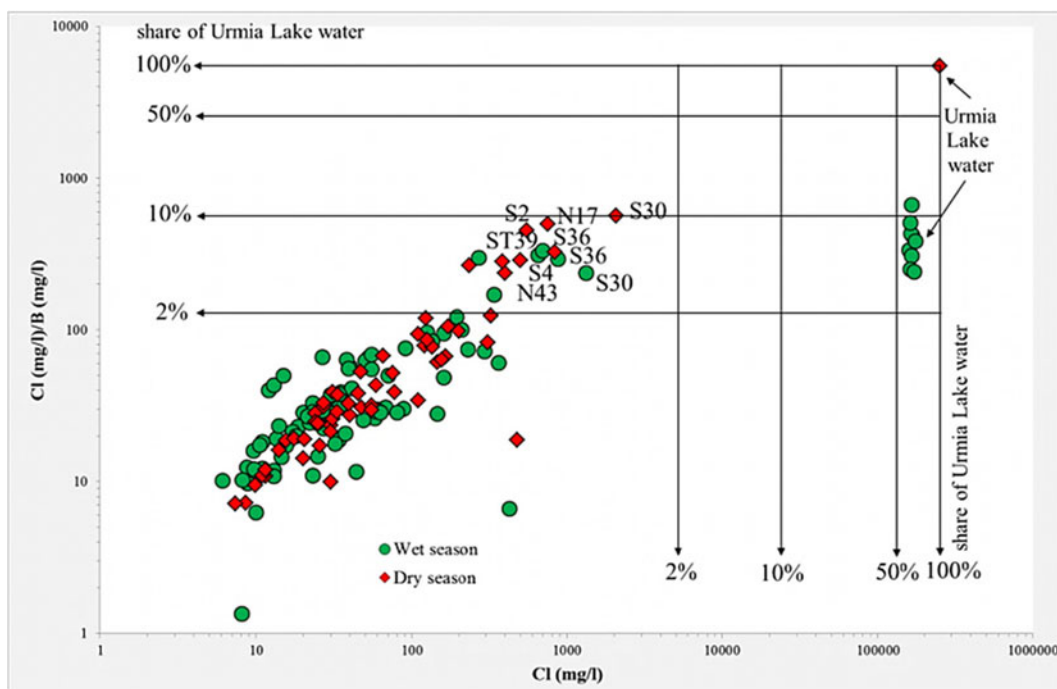


Fig. 8 Changes of Cl^-/B ratio versus Cl^- concentration in groundwater and UL samples

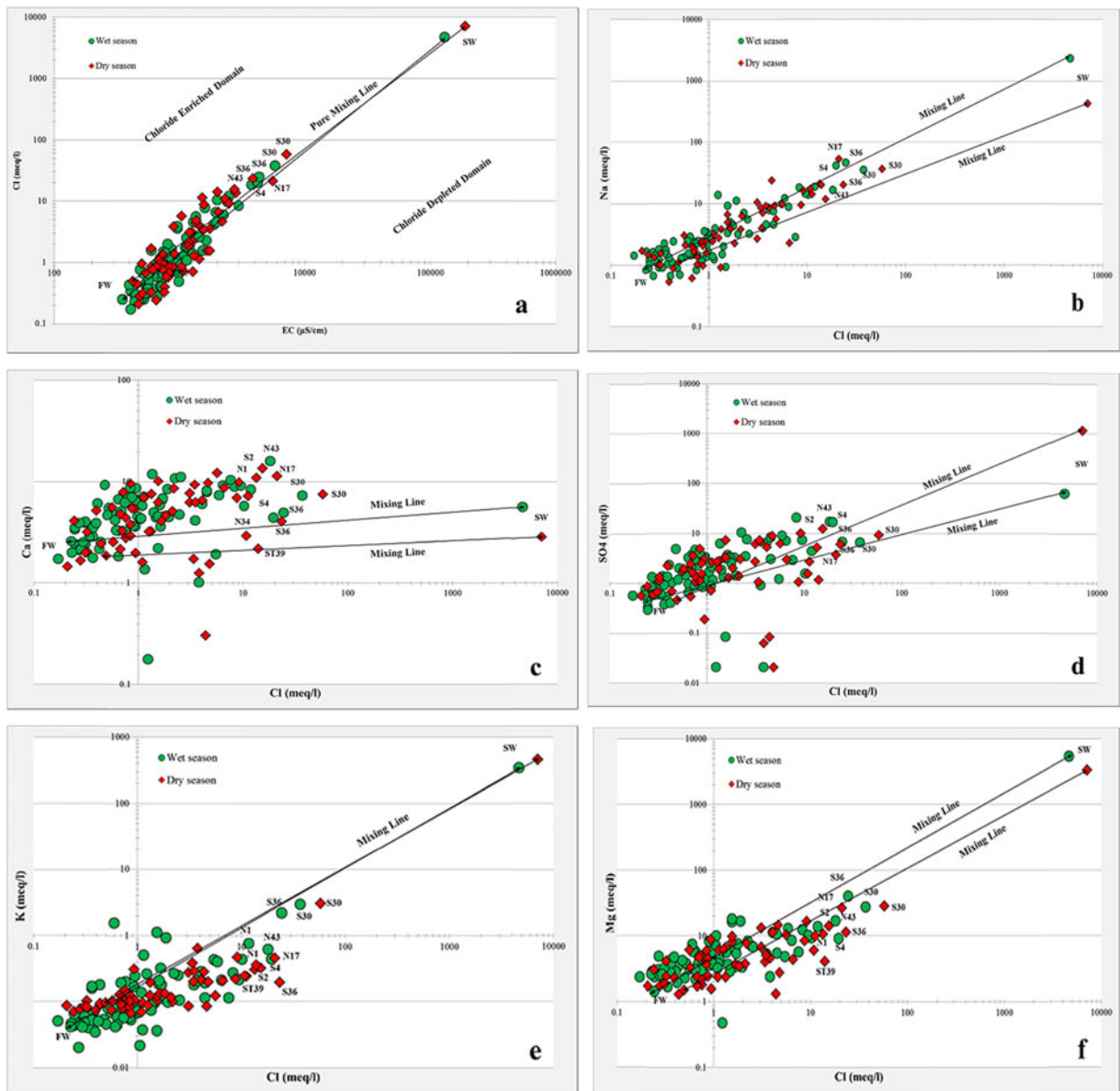


Fig. 9 Relationships between the concentrations of Cl^- and **a** EC, **b** Na^+ , **c** Ca^{2+} , **d** SO_4^{2-} , **e** K^+ , and **f** Mg^{2+} in groundwater samples collected in the Urmia plain for wet and dry seasons. Concentrations expressed in milliequivalents per liter

may also be important. Often, the chemical composition of salinized groundwater does not indicate a single source or salinization mechanism, given similarities in the chemical compositions of different saline sources.

One of the main approaches to evaluation of some salinity sources is using different ions to chloride ratios such as Na^+/Cl^- and $\text{Ca}^{2+}/\text{Cl}^-$ ratios. For example, saltwater encroachment into coastal aquifers is associated with an inverse correlation between Na^+/Cl^- and $\text{Ca}^{2+}/\text{Cl}^-$ due to ion exchange reactions, resulting in low Na^+

Cl^- and high $\text{Ca}^{2+}/\text{Cl}^-$ ratios relative to saltwater values. In contrast, non-marine/salt lake salinity sources typically have $\text{Na}^+/\text{Cl}^- > 1$. The Na^+/Cl^- ratio can be changed by water-rock interaction and ion exchange reactions. Therefore, these processes can reduce the Na^+/Cl^- ratio of saline/saltwater in non-marine/salt lake settings. The relationship between the Na^+ and Cl^- (Fig. 9b) suggests a pattern that closely follows the blending process characterized by the conservative mixing lines, even though some deviations from the lines were recorded. Generally,

change of Na^+ vs. Cl^- is a good tracer to distinguish different sources of salinity. However, the reactivity of Na^+ in the unsaturated zone can reduce the Na^+/Cl^- ratio. It is, therefore, essential to use assemblages of diagnostic chemical tracers for accurate delineation of the salinity sources. The samples with low concentration of Na^+ showed the high Ca^{2+} content and vice versa. Thus, the major ion concentrations (Ca^{2+} , Na^+ , and Cl^-) cannot be explained by the simple mixing of freshwater and saltwater. It seems that a combination of factors particularly water-rock interaction with carbonate rocks and clay materials is the controlling mechanism of mineralization in these groundwater samples.

The distribution of Ca^{2+} vs. Cl^- concentration (Fig. 9c) shows the more dispersion than other ions. In addition, some saline samples (e.g., S30, N17, N43, S4, S2, and N1) contained the high values of Ca^{2+} with respect to the conservative mixing line.

The relationship between SO_4^{2-} and Cl^- concentration represented in Fig. 9d indicates that concentration of SO_4^{2-} is generally determined by the presence of UL saltwater, although some samples displayed a higher concentration than expected (points near the SW end member). The intrusion of saltwater into coastal aquifers is also associated with redox conditions along the saltwater-freshwater interface. Thus, saline groundwater samples associated with saltwater intrusion are characterized by low $\text{SO}_4^{2-}/\text{Cl}^-$ ratios (Krouse and Mayer 2000).

The behavior of K^+ (Fig. 9e) indicates that while the K^+ content of the fresher waters was consistent with the conservative mixing lines, the saline groundwater samples had lower potassium values. It seems that ion exchange processes are very important mechanisms in determining the ionic content of the coastal groundwater in this aquifer. In this part, the more saline groundwater fell below the conservative mixing lines.

Based on Fig. 9f, there is a relatively good correlation between Mg^{2+} and Cl^- . In this figure, like the Fig. 9e, the saline groundwater samples are located below the conservative mixing lines.

In this research, the ionic deltas for Mg^{2+} , Na^+ , and Ca^{2+} as major cations in water samples were plotted versus chloride concentration (Fig. 10a, b) to recognize the processes that can change the theoretical content and to identify the behavior of these cations in groundwater samples. In the wet season, the majority of samples such as S30, S36, S4, N43, N1, N2, and S2 are depleted in Mg^{2+} and Na^+ and relatively enriched in Ca^{2+} . The loss of Na^+ and gain of Ca^{2+} exhibit a direct cation exchange

generally occurred in situations when the saline/saltwater is replacing fresh groundwater (Appelo and Postma 2005; Kouzana et al. 2009; Zghibi et al. 2013). Generally, the depletion of Mg^{2+} and enrichment of Ca^{2+} show a possible exchange reaction between these two cations. There is the absorption of Mg^{2+} and a release of Ca^{2+} from the clay minerals in the case of salinization while the reverse occurs in the case of dilution (desalinization) in some samples. As shown in Fig. 10, the ionic deltas for Mg^{2+} , Na^+ , and relatively Ca^{2+} in the dry season are more than wet season. Therefore, it can be expected that the groundwater samples get enriched for these ions compared to the theoretical mixing.

In Fig. 11, all salinization factors in the coastal groundwater samples are presented as the saltwater percentage. In both wet and dry seasons, sample S33 with the lowest content of Cl^- is considered as representative of freshwater. The percentage of saltwater in the groundwater samples is very low, ranging between 0.001 % (S31) and 0.79 % (S30) in the wet season and 0.0004 % (N19) and 0.81 % (S30) in the dry season.

The methods discussed in the previous sections are useful for understanding the dynamics of saltwater encroachment. The use of some diagrams such as Piper diagram does not allow for a precise analysis of the facies evolution during saline/saltwater encroachment and freshening phases. Giménez-Forcada (2010) has recommended the HFE diagram as a useful tool for this purpose. The position of water samples on the HFE diagram is presented in Fig. 12.

The freshwaters belong to the $\text{Ca-HCO}_3/\text{SO}_4$ (13), and saline waters show the Na-Cl facies (4). In both wet and dry seasons, most of the groundwater samples followed the succession of facies along the mixing line (4→7→10→13), which exhibits simple mixing with little or no intervention of ion exchange reactions. During the encroachment phase, to the right and beneath horizontal line 33.3 %, the Ca-Cl facies (16) can be formed because of increase in salinity and reverse cation exchange of $\text{Na}^+/\text{Ca}^{2+}$ (13→14→15→16). In this study, the presence of two samples (N11, S3) in parts 15 and 16 (in the wet season) and sample S2 in part 15 (in the dry season) show that the facies was influenced by reverse ion exchange reactions ($\text{Na}^+/\text{Ca}^{2+}$). This type of water evolves toward facies that is closer to saline water (Na-Cl) (4) (16→12→8→4). In the freshening phase, the direct ion exchange processes occur more slowly. Under this condition, the water gains Na^+

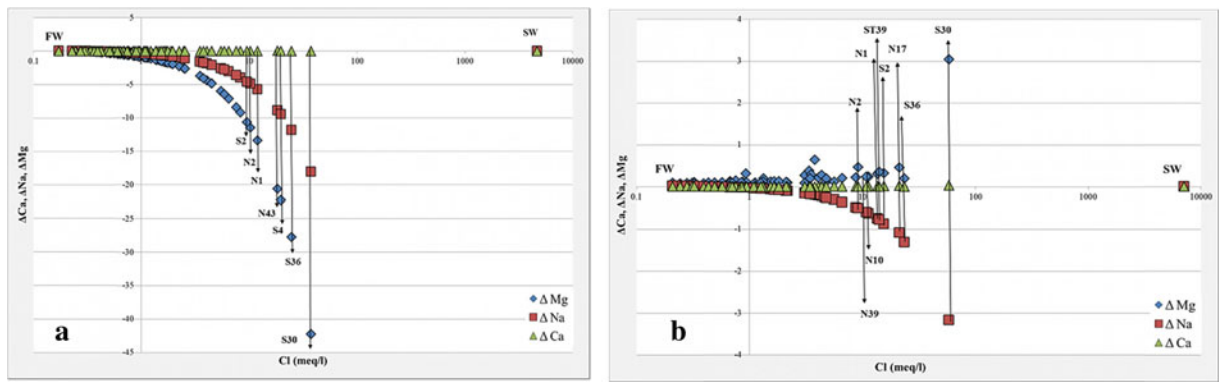


Fig. 10 Changes of ΔMg^{2+} , ΔNa^+ , and ΔCa^{2+} versus Cl^- of groundwater samples in **a** wet and **b** dry seasons

and releases Ca^{2+} until $Na-HCO_3/SO_4$ facies (1) is achieved ($4 \rightarrow 3 \rightarrow 2 \rightarrow 1$). In the Urmia area, locating some samples (black points) in parts 1 and 2 shows the overlapping in mixing line between fresh groundwater and saltwater caused by direct ion exchange process. In the coastal parts of UA, the facies $Na-HCO_3/SO_4$ (1), $Na-MixHCO_3/MixSO_4$ (2), $MixNa-HCO_3/SO_4$ (5), and $MixNa-MixHCO_3/MixSO_4$ (6) are reached in the wet season. In the dry season, only the facies $Na-HCO_3/SO_4$ (1) and $Na-MixHCO_3/MixSO_4$ (2) are reached.

According to Fig. 12 and Table 5 which presents hydrochemical facies of Urmia groundwater samples based on the HFE diagram, the most samples that collected repeatedly in both wet and dry seasons showed the same hydrochemical facies, which indicate that the seasonal groundwater fluctuations cannot significantly change the chemical composition of groundwater. In general, this situation is observed in wells that are far from the UL (parts 9, 10, 13, and 14 in HFE-D) and have the $MixCa-HCO_3$, $MixCa-MixHCO_3$, $Ca-HCO_3$, and $Ca-MixHCO_3$ water facies.

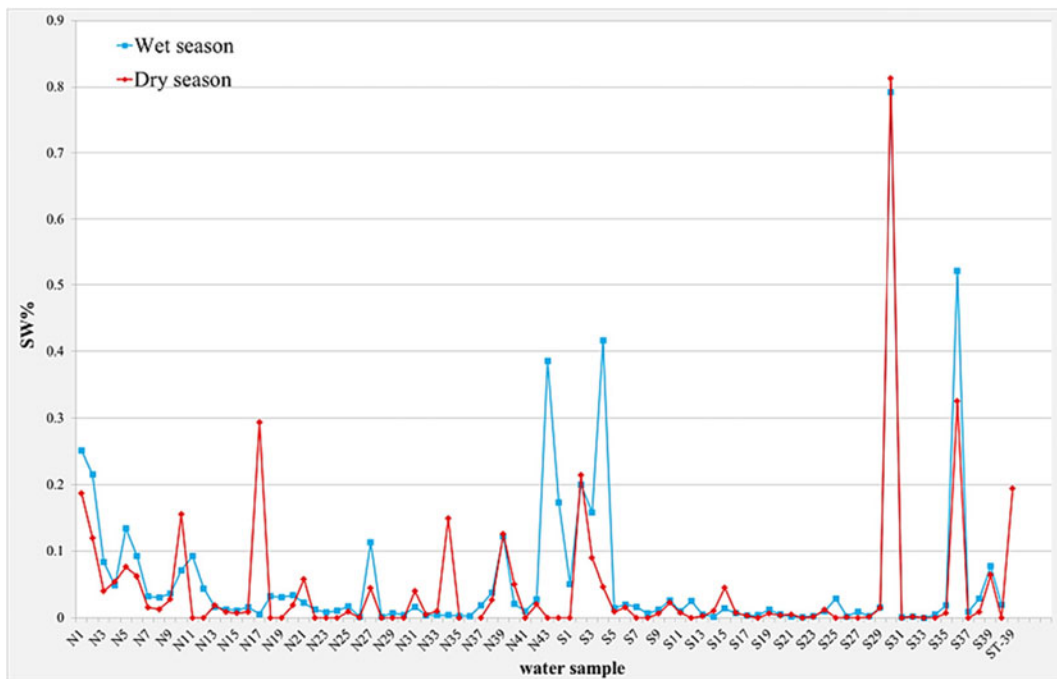


Fig. 11 Percentage of saltwater in groundwater samples relative to salinity of UL

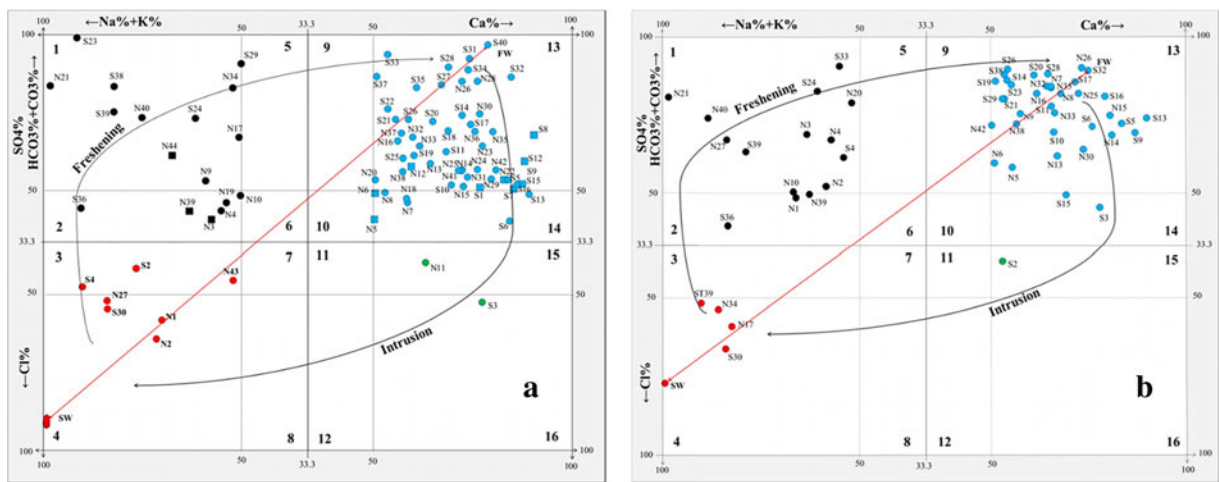


Fig. 12 HFE diagram for Urmia groundwater samples in **a** wet and **b** dry seasons (*N#*, *S#*: samples collected in the northern and southern parts of the Urmia plain; *square symbol*: SO_4^{2-} water in

freshening stage; *ST39* and *S39* are sampled at the same location, *ST39* from the upper unconfined aquifer, and *S39* from confined aquifer)

Table 5 Hydrochemical facies of groundwater samples based on HFE diagram in wet and dry seasons

Period	Sample location	HFE facies	No. of sample	Percent
Wet season (June 2014)	Northern part (N samples)	Na-HCO ₃ /SO ₄	6	13.64
		Na-MixHCO ₃ /MixSO ₄	5	11.36
		Na-MixCl	1	2.27
		Na-Cl	3	6.82
		Ca-HCO ₃ /SO ₄	23	52.27
		Ca-MixHCO ₃ /MixSO ₄	5	11.36
		Ca-MixCl	1	2.27
	Total	44	100	
	Southern part (S samples)	Na-HCO ₃ /SO ₄	5	12.50
		Na-MixHCO ₃ /MixSO ₄	1	2.50
		Na-MixCl	2	5
		Na-Cl	1	2.50
		Ca-HCO ₃ /SO ₄	28	70
		Ca-MixHCO ₃ /MixSO ₄	2	5
Ca-Cl		1	2.50	
Total	40	100		
Dry season (September 2014)	Northern part (N samples)	Na-HCO ₃ /SO ₄	8	28.58
		Na-MixHCO ₃ /MixSO ₄	2	7.14
		Na-Cl	2	7.14
		Ca-HCO ₃ /SO ₄	16	57.14
	Total	28	100	
	Southern part (S samples)	Na-HCO ₃ /SO ₄	4	13.79
		Na-MixHCO ₃ /MixSO ₄	1	3.45
		Na-Cl	2	6.90
		Ca-HCO ₃ /SO ₄	19	65.52
		Ca-MixHCO ₃ /MixSO ₄	2	6.90
Ca-MixCl		1	3.45	
Total	29	100		

Results of Table 5 show that about 52.27 and 57.14 % of samples collected from the northern part of UA have Ca-HCO₃/SO₄ facies for wet and dry seasons, respectively. In addition, 70 and 65.52 % of groundwater samples of southern part show the Ca-HCO₃/SO₄ facies for wet and dry seasons, respectively.

Conclusion

We studied the potential salinity originated from UL in the Urmia coastal aquifer using a combination of hydrogeological and hydrochemical measurements. The relationship between the concentrations of some major ions and Cl⁻ is relatively consistent with conservative mixing line, and just some samples showed the salty composition related with UL. The behaviors of Ca²⁺ and Na⁺ show the involvement of ionic exchange between the saline water and solid fraction of the aquifer (water-rock interaction). This interpretation was largely confirmed by applying the HFE diagram, which further helped to characterize the process of saltwater intrusion, as well as elucidating the evolution and dynamics of the saline front (saltwater intrusion or freshening phases) within the aquifer. The plots of water samples on HFE-D indicate that 52.27 and 57.14 % of groundwater samples collected from the northern part of UA in wet and dry seasons, respectively, have Ca-HCO₃/SO₄ facies. In addition, 70 and 65.52 % of groundwater samples of southern part show the Ca-HCO₃/SO₄ facies for these seasons. The hydrochemical evidence indicates that except for a few wells near the coast, there is a little hydraulic interaction between UA and UL.

Acknowledgments This work is financially supported by Geological Survey of Iran (GSI). We thank all members of GSI for their kind cooperation that made this research possible. The authors would like to thank the anonymous reviewers for their constructive comments. We also like to thank the Prof. Yu-Pin Lin, associate editor of EMAS journal, for his helpful comments and support during the review process.

Compliance with ethical standards This study was funded by the Geological Survey of Iran (GSI).

For this type of study, formal consent is not required.

This article does not contain any studies with human participants or animals performed by any of the authors.

Conflict of interest The authors declare that they have no conflict of interest.

References

- Amiri, V., Rezaei, M., & Sohrabi, N. (2014). Groundwater quality assessment using entropy weighted water quality index (EWQI) in Lenjanat, Iran. *Environmental Earth Sciences*, 72, 3479–3490.
- Amiri, V., Sohrabi, N., & Altafi Dadgar, M. (2015). Evaluation of groundwater chemistry and its suitability for drinking and agricultural uses in the Lenjanat plain, central Iran. *Environmental Earth Sciences*, 74, 6163–6176.
- Andersen, M. S., Jakobsen, V. N. R., & Postma, D. (2005). Geochemical processes and solute transport at the seawater/freshwater interface of a sandy aquifer. *Geochimica et Cosmochimica Acta*, 69, 3979–3994.
- APHA (American Public Health Association), (1985). *Standard methods of the examination of water/wastewater* (16th ed.). New York: APHA, AWWA, and WPCF.
- Appelo, C. A. J., & Postma, D. (2005). *Geochemistry, groundwater and pollution*. 2nd edition, CRC Press.
- Asfahani, J., & Abou Zakhem, B. (2013). Geoelectrical and hydrochemical investigations for characterizing the salt water intrusion in the Khanasser valley, Northern Syria. *Acta Geophysica*, 61(2), 422–444.
- Barker, A. P., Newton, R. J., & Bottrell, S. H. (1998). Processes affecting groundwater chemistry in a zone of saline intrusion into an urban aquifer. *Applied Geochemistry*, 13, 735–749.
- Barlow, P. M., & Reichard, E. G. (2010). Saltwater intrusion in coastal regions of North America. *Hydrogeology Journal*, 18, 247–260.
- Bear, J., Cheng, A. H. D., Sorek, S., Ouazar, D., & Herrera, I. (Eds.) (2013). *Seawater intrusion in coastal aquifers: concepts, methods and practices*. Springer Science & Business Media.
- Boluda-Botella, N., Valdes-Abellan, J., & Pedraza, R. (2014). Applying reactive models to column experiments to assess the hydrogeochemistry of seawater intrusion: optimising ACUAINTRUSION and selecting cation exchange coefficients with PHREEQC. *Journal of Hydrology*, 510, 59–69.
- Bouzourra, H., Bouhlila, R., Elango, L., Slama, F., & Ouslati, N. (2015). Characterization of mechanisms and processes of groundwater salinization in irrigated coastal area using statistics, GIS, and hydrogeochemical investigations. *Environmental Science and Pollution Research*, 22(4), 2643–2660.
- Buschmann, J., & Berg, M. (2009). Impact of sulfate reduction on the scale of arsenic contamination in groundwater of the Mekong, Bengal and Red River deltas. *Applied Geochemistry*, 24, 1278–86.
- Carreira, P. M., Marques, J. M., & Nunes, D. (2014). Source of groundwater salinity in coastline aquifers based on environmental isotopes (Portugal): natural vs. human interference. A review and reinterpretation. *Applied Geochemistry*, 41, 163–175.
- Cary, L., Petelet-Giraud, E., Bertrand, G., Kloppmann, W., Aquilina, L., Martins, V., Hirata, R., Montenegro, S., Pauwels, H., Chatton, E., Franzen, M., Aurouet, A., Lasseur, E., Picot, G., Guerrot, C., Fléhoc, C., Labasque, T., Santos, J. G., Paiva, A., Braibant, G., & Pierre, D. (2015). Origins and processes of groundwater salinization in the urban coastal aquifers of Recife (Pernambuco, Brazil): a

- multi-isotope approach. *Science of the Total Environment*, 530–531, 411–429.
- Chen, K., & Jiao, J. J. (2014). Modeling freshening time and hydrochemical evolution of groundwater in coastal aquifers of Shenzhen, China. *Environmental Earth Sciences*, 71, 2409–2418.
- Chen, K., Jiao, J., Huang, J., & Huang, R. (2007). Multivariate statistical evaluation of trace elements in groundwater in a coastal area in Shenzhen, China. *Environmental Pollution*, 147, 771–780.
- Choudhury, K., Saha, D. K., & Chakraborty, P. (2001). Geophysical study for saline water intrusion in a coastal alluvial terrain. *Journal of Applied Geophysics*, 46, 189–200.
- Cimino, A., Cosentino, C., Oieni, A., & Tranchina, L. (2008). A geophysical and geochemical approach for seawater intrusion assessment in the Acquedolci coastal aquifer (Northern Sicily). *Environmental Geology*, 55, 1473–1482.
- El Yaouti, F., El Mandour, A., Khattach, D., Benavente, J., & Kaufmann, O. (2009). Salinization processes in the unconfined aquifer of Bou-Areg (NE Morocco): a geostatistical, geochemical, and tomographic study. *Applied Geochemistry*, 24, 16–31.
- Esmacili-Vardanani, M., Rasa, I., Amiri, V., Yazdi, M., & Pazand, K. (2015). Evaluation of groundwater quality and assessment of scaling potential and corrosiveness of water samples in Kadkan aquifer, Khorasan-e-Razavi Province, Iran. *Environmental Monitoring and Assessment*, 187, 53. doi: 10.1007/s10661-014-4261-0.
- Fidelibus, M. D. (2003). Environmental tracing in coastal aquifers: old problems and new solutions. In *Coastal aquifers intrusion technology: Mediterranean countries* (Vol. II, pp. 79–111). Madrid: Publ. IGME.
- Ged, E. C. (2013). Saltwater intrusion impacts on bromide concentration and disinfection byproduct formation: model evaluation and laboratory scale analysis. Master thesis, University of Florida.
- Gerritse, R. G., & George, R. J. (1988). The role of soil organic matter in the geochemical cycling of chloride and bromide. *Journal of Hydrology*, 101(1–4), 83–95.
- Ghiglieri, G., Carletti, A., & Pittalis, D. (2012). Analysis of salinization processes in the coastal carbonate aquifer of Porto Torres (NW Sardinia, Italy). *Journal of Hydrology*, 432–433, 43–51.
- Gibbs, R. J. (1970). Mechanisms controlling world water chemistry. *Science*, 17, 1088–1090.
- Giménez-Forcada, E. (2010). Dynamic of sea water interface using hydro chemical facies evolution diagram. *Ground Water*, 48(2), 212–216.
- Goldberg, S., & Kabengi, N. J. (2010). Bromide adsorption by reference minerals and soils. *Vadose Zone Journal*, 9, 780–786.
- Gurunadha Rao, V. V. S., Tamma Rao, G., Surinaidu, L., Mahesh, J., Mallikharjuna Rao, S. T., & Mangaraja Rao, B. (2013). Assessment of geochemical processes occurring in groundwaters in the coastal alluvial aquifer. *Environmental Monitoring and Assessment*, 185, 8259–8272.
- Han, D. M., Song, X. F., Currell, M. J., Yang, L., & Xiao, G. Q. (2014). Chemical and isotopic constraints on evolution of groundwater salinization in the coastal plain aquifer of Laizhou Bay, China. *Journal of Hydrology*, 508, 12–27.
- Harman, H. H. (1960). *Modern factor analysis*. University of Chicago Press.
- Helena, B., Pardo, R., Vega, M., Barrado, E., Fernandez, J. M., & Fernandez, L. (2000). Temporal evolution of groundwater composition in an alluvial aquifer (Pisuerga River, Spain) by principal component analysis. *Water Research*, 34, 807–816.
- ISO (International Standards Organisation) (1993). Water quality—sampling—part 11: guidance on sampling of ground waters. ISO 5667-11.
- Jones, B. F., Vengosh, A., Rosenthal, E., & Yechieli, Y. (1999). Geochemical investigations. In J. Bear, A. H. D. Cheng, S. Soreq, D. Ouazar, & I. Herrera (Eds.), *Seawater intrusion in coastal aquifers—concepts, methods and practices*, ch. 3 (pp. 51–72). Dordrecht: Kluwer Academic.
- Jorgensen, N. O., Andersen, M. S., & Engesgaard, P. (2008). Investigation of a dynamic seawater intrusion event using strontium isotopes ($^{87}\text{Sr}/^{86}\text{Sr}$). *Journal of Hydrology*, 348, 257–269.
- Kaiser, H. F. (1958). The varimax criteria for analytical rotation in factor analysis. *Psychometrika*, 23, 187–200.
- Kamei, T., Ikeda, J., Ishida, H., Ismda, S., Onishi, I., Partoazar, H., Sasajima, S., & Nishimur, S. (1973). A general report on the geological and paleontological survey in Maragheh Area, North-West Iran. Internal Report, Geological Survey of Iran.
- Katz, B. G., Eberts, S. M., & Kauffman, L. J. (2011). Using Cl/Br ratios and other indicators to assess potential impacts on groundwater quality from septic systems: a review and examples from principal aquifers in the United States. *Journal of Hydrology*, 397, 151–166.
- Kim, K. Y., Park, Y. S., Kim, G. P., & Park, K. H. (2009). Dynamic fresh water-saline water interaction in the coastal zone of Jeju Island, South Korea. *Hydrogeology Journal*, 17, 617–629.
- Kouzana, L., Ben Mammou, A., & Sfar Felfoul, M. (2009). Seawater intrusion and associated processes: case of the Korba aquifer (Cap-Bon, Tunisia). *Comptes Rendus Geoscience*, 341, 21–35.
- Krouse, H. R., & Mayer, B. (2000). Sulphur and oxygen isotopes in sulphate. In P. Cook & A. L. Herczeg (Eds.), *Environmental tracers in subsurface hydrology* (pp. 195–231). Boston: Kluwer Academic.
- Langman, J. B., & Ellis, A. S. (2010). A multi-isotope (δD , $\delta^{18}\text{O}$, $^{87}\text{Sr}/^{86}\text{Sr}$ and $\delta^{11}\text{B}$) approach for identifying saltwater intrusion and resolving groundwater evolution along the Western Caprock Escarpment of the Southern High plains, New Mexico. *Applied Geochemistry*, 25, 159–174.
- Lee, J. Y., & Song, S. H. (2007). Evaluation of groundwater quality in coastal areas: implications for sustainable agriculture. *Environmental Geology*, 52(7), 1231–1242.
- Li, J., He, M., Han, W., & Gu, Y. (2009). Analysis and assessment on heavy metal sources in the coastal soils developed from alluvial deposits using multivariate statistical methods. *Journal of Hazardous Materials*, 164, 976–981.
- Liu, C. W., Lin, K. H., & Kuo, Y. M. (2003). Application of factor analysis in the assessment of groundwater quality in a black-foot disease area in Taiwan. *Science of the Total Environment*, 313, 77–89.
- Lowers, H. A., Breit, G. N., Foster, A. L., Whitney, J., Yount, J., Uddin, M. N., & Muneem, A. A. (2007). Arsenic incorporation into authigenic pyrite, Bengal Basin sediment, Bangladesh. *Geochimica et Cosmochimica Acta*, 71, 2699–717.
- Lucas, Y., Schmitt, A. D., Chabaux, F., Clément, A., Fritz, B., Elsass, P., & Durand, S. (2010). Geochemical tracing and hydrogeochemical modelling of water-rock interactions

- during salinization of alluvial groundwater (Upper Rhine Valley, France). *Applied Geochemistry*, 25, 1644–1663.
- Mandilaras, D., Lambrakis, N., & Stamatis, G. (2008). The role of bromide and iodide ions in the salinization mapping of the aquifer of Glafkos River basin (northwest Achaia, Greece). *Hydrological Processes*, 22, 611–622.
- Manno, E., Vassallo, M., Varrica, D., Dongarrà, G., & Hauser, S. (2006). Hydrogeochemistry and water balance in the coastal wetland area of “Biviere di Gela”, Sicily, Italy. *Water, Air, and Soil Pollution*, 178(1–4), 179–193.
- Martinez, R., Sánchez-Mata, D., & Costa, M. (1999). Boreal and western temperate forest vegetation (syntaxonomical synopsis of the potential natural plant communities of North America II). *Itinera Geobotanica*, 12, 3–311.
- Matiatos, I., Alexopoulos, A., & Godelitsas, A. (2014). Multivariate statistical analysis of the hydrogeochemical and isotopic composition of the groundwater resources in northeastern Peloponnesus (Greece). *Science of the Total Environment*, 476–477, 577–590.
- McArthur, J. M., Sikdar, P. K., Hoque, M. A., & Ghosal, U. (2012). Waste-water impacts on groundwater: Cl/Br ratios and implications for arsenic pollution of groundwater in the Bengal Basin and Red River Basin, Vietnam. *Science of the Total Environment*, 437, 390–402.
- Melloul, A., & Collin, M. (2006). Hydrogeological changes in coastal aquifers due to sea level rise. *Ocean and Coastal Management*, 49, 281–297.
- Ministry of Energy (2010). Integrated management plan for Lake Urmia Basin. Internal report, 91pp.
- Mollema, P. N., Antonellini, M., Dinelli, E., Gabbianelli, G., Greggio, N., & Stuyfzand, P. J. (2013). Hydrochemical and physical processes influencing salinization and freshening in Mediterranean low-lying coastal environments. *Applied Geochemistry*, 34, 207–221.
- Mondal, N. C., Singh, V. S., Puranik, S. C., & Singh, V. P. (2010). Trace element concentration in groundwater of Pesarlanka Island, Krishna Delta, India. *Environmental Monitoring and Assessment*, 163(1–4), 215–227.
- Mondal, N. C., Singh, V. P., Singh, S., & Singh, V. S. (2011). Hydrochemical characteristic of coastal aquifer from Tuticorin, Tamil Nadu, India. *Environmental Monitoring and Assessment*, 175, 531–550.
- Mongelli, G., Monni, S., Oggiano, G., Paternoster, M., & Sinisi, R. (2013). Tracing groundwater salinization processes in coastal aquifers: a hydrogeochemical and isotopic approach in the Na-Cl brackish waters of northwestern Sardinia, Italy. *Hydrology and Earth System Sciences*, 17, 2917–2928.
- Morell, I., Medina, J., Pulido-Bosch, A., & Fernández-Rubio, R. (1986). The use of bromide and strontium as indicators of marine intrusion in the aquifer of Oropesa-Torreblanca. Castellón. Spain. Proc. 9th. Salt Water Intrusion Meeting, Delft, Denmark 61–72.
- Morell, I., Pulido-Bosch, A., Sanchez-Martos, F., Vallejos, A., Daniele, L., Calaforra, J. M., Roig, A. F., & Renau, A. (2008). Characterization of the salinisation processes in aquifers using boron isotopes; application to South-Eastern Spain. *Water, Air, & Soil Pollution*, 187, 65–80.
- Morrow, F. J., Ingham, M. R., & McConchie, J. A. (2010). Monitoring of tidal influences on the saline interface using resistivity traversing and cross-borehole resistivity tomography. *Journal of Hydrology*, 389, 69–77.
- Nakhaei, M., Amiri, V., Rezaei, K., & Moosaei, F. (2015). An investigation of the potential environmental contamination from the leachate of the Rasht waste disposal site in Iran. *Bulletin of Engineering Geology and the Environment*, 74, 233–246.
- NOAA (National Oceanic and Atmospheric Administration). (2012). Oroomieh climate normals 1961–1990. Retrieved December 27.
- Ozler, H. M. (2003). Hydrochemistry and salt-water intrusion in the Van aquifer, East Turkey. *Environmental Geology*, 43, 759–775.
- Panno, S. V., Hackley, K. C., Hwang, H. H., Greenberg, S. E., Krapac, I. G., Landsberger, S., & O’Kelly, D. J. (2006). Characterization and identification of Na-Cl sources in groundwater. *Ground Water*, 44, 176–187.
- Parkhurst, D. L., & Appelo, C. A. J. (1999). User’s guide to PHREEQC (version 2), a computer program for speciation, batch-reaction, one-dimensional transport and inverse geochemical calculations. US Geological Survey, Water-Resources Investigations Report 99–4259.
- Petelet-Giraud, E., Négrel, P., Guerrot, C., Aunay, B., & Dörfliger, N. (2013). Origins and processes of salinization of a Plio-Quaternary coastal Mediterranean multilayer aquifer: the Roussillon Basin case study. *Procedia Earth and Planetary Science*, 7, 681–684.
- Rodellas, V., Garcia-Orellana, J., Garcia-Solsona, E., Masqué, P., Antonio Domínguez, J., Ballesteros, B. J., Mejías, M., & Zarroca, M. (2012). Quantifying groundwater discharge from different sources into a Mediterranean wetland by using ²²²Rn and Ra isotopes. *Journal of Hydrology*, 466–467, 11–22.
- Russak, A., & Sivan, O. (2010). Hydrogeochemical tool to identify salinization or freshening of coastal aquifers determined from combined field work, experiments, and modeling. *Environmental Science & Technology*, 44(11), 4096–4102.
- Sartipi, A. H., Haghfarshi, E., Karimi, H., Shiva, E., Seidi Sahbari, P., Vakil Baghmisheh, F., & Zamani mehr, S. (2014). Geological report of the Urmia map (1:25000); 5065 III SW. (In Persian).
- Saxena, V. K., Mondal, N. C., & Singh, V. S. (2004). Identification of seawater ingress using Sr and B in Krishna delta. *Current Science*, 86(4), 586–590.
- Sayles, F. L., & Mangelsdorf, P. C., Jr. (1977). The equilibration of clay minerals with sea water: exchange reactions. *Geochimica et Cosmochimica Acta*, 41, 951–960.
- Schiavo, M. A., Hauser, S., & Povinec, P. P. (2009). Stable isotopes of water as a tool to study groundwater-seawater interactions in coastal south-eastern Sicily. *Journal of Hydrology*, 364, 40–49.
- Schroeder, R. A., & Rivera, M. (1993). Physical, chemical and biological data for detailed study of irrigation drainage in the Salton Sea area, California. US Geological Survey Open-File report 93–83. Menlo Park, CA: US Geological Survey.
- Schryer, D. R. (1982). Heterogeneous atmospheric chemistry. *American Geophysical Union*, 28
- Seaman, J. C., Bertsch, P. M., Korom, S. F., & Miller, W. P. (1996). Physicochemical controls on nonconservative anion migration in coarse-textured alluvial sediments. *Ground Water*, 34(5), 778–783.
- Singh, V. S., Sarwade, D. V., Mondal, N. C., Nanadakumar, M. V., & Singh, B. (2009). Evaluation of groundwater resources in a tiny Andrott Island, Union Territory of Lakshadweep, India. *Environmental Monitoring and Assessment*, 158(1–4), 145–154.

- Skrzypek, G., Dogramaci, S., & Grierson, F. P. (2013). Geochemical and hydrological processes controlling groundwater salinity of a large inland wetland of northwest Australia. *Chemical Geology*, 357, 164–177.
- Terzić, J., Markovic, T., & Pekas, Z. (2008). Influence of seawater intrusion and agricultural production on the Blato Aquifer, Island of Korčula, Croatia. *Environmental Geology*, 54, 719–729.
- Tomaszkiewicz, M., Abou Najm, M., & El-Fadel, M. (2014). Development of a groundwater quality index for seawater intrusion in coastal aquifers. *Environmental Modelling & Software*, 57, 13–26.
- Vandenbohede, A., & Lebbe, L. (2012). Groundwater chemistry patterns in the phreatic aquifer of the central Belgian coastal plain. *Applied Geochemistry*, 27, 22–36.
- Vengosh, A. (2014). Salinization and saline environments. *Treatise on Geochemistry (Second Edition)*, 11, 325–378.
- Ward, J. H., Jr. (1963). Hierarchical grouping to optimize an objective function. *Journal of the American Statistical Association*, 58(301), 236–244.
- Warner, N. R., Lgourma, Z., Bouchaou, L., Boutaleb, S., Tagmab, T., Hsaissouneb, M., & Vengosha, A. (2013). Integration of geochemical and isotopic tracers for elucidating water sources and salinization of shallow aquifers in the sub-Saharan Drâa Basin, Morocco. *Applied Geochemistry*, 34, 140–151.
- Whittemore, D. O., & Davis, S. N. (1995). Patterns of Cl/Br with Cl concentration in the hydrosphere. *Geological Society of America Abstracts with Programs*, 27(6), 465–466.
- Wilson, S. R., Ingham, M., & McConchie, J. A. (2006). The applicability of earth resistivity methods for saline interface definition. *Journal of Hydrology*, 316, 301–312.
- WMO (World Meteorological Organisation). (2014). <http://worldweather.wmo.int/en/city.html?cityId=1454>
- World Health Organization (2011). Guidelines for drinking-water quality. 4th ed. Available: http://www.who.int/water_sanitation_health/publications/2011/dwq_chapters/en/.
- Yechieli, Y., Kafri, U., & Sivan, O. (2009). The inter-relationship between coastal sub-aquifers and the Mediterranean Sea, deduced from radioactive isotopes analysis. *Hydrogeology Journal*, 17, 265–274.
- Yidana, S. M., Ophori, D., & Banoeng-Yakubo, B. (2008). A multivariate statistical analysis of surface water chemistry data—the Ankobra Basin, Ghana. *Journal of Environmental Management*, 86(1), 80–87.
- Zghibi, A., Zouhri, L., Tarhouni, J., & Kouzana, L. (2013). Groundwater mineralisation processes in Mediterranean semiarid systems (Cap-Bon, North east of Tunisia): hydrogeological and geochemical approaches. *Hydrological Processes*, 27(22), 3227–3233.
- Zhang, X., Qian, H., Chen, J., & Qiao, L. (2014). Assessment of groundwater chemistry and status in a heavily used semi-arid region with multivariate statistical analysis. *Water*, 6(8), 2212–2232.